RSC Advances

REVIEW

View Article Online
View Journal | View Issue

Cite this: *RSC Adv.*, 2025, **15**, 7018

Recent advances in the synthesis of anticancer pyrazole derivatives using microwave, ultrasound, and mechanochemical techniques

Diana Becerra* and Juan-Carlos Castillo *

Pyrazole and its derivatives have attracted considerable attention in pharmaceutical and medicinal chemistry, as reflected in their presence in numerous FDA-approved drugs and clinical candidates. This review presents a comprehensive analysis of articles published between 2014 and 2024, focusing on the microwave-, ultrasound-, and mechanochemical-assisted synthesis of pyrazole derivatives with anticancer activity. It explores synthetic methodologies, anticancer efficacy, and molecular docking studies, underscoring the significance of pyrazole derivatives in drug discovery and medicinal chemistry. Notably, microwave irradiation stands out as the most widely employed technique, providing high efficiency by significantly reducing reaction times while maintaining moderate temperatures. Ultrasound irradiation serves as a valuable alternative, particularly for processes that require milder conditions, whereas mechanochemical activation, though less frequently employed, offers distinct advantages in terms of sustainability.

Received 18th December 2024
Accepted 21st February 2025

DOI: 10.1039/d4ra08866b

rsc.li/rsc-advances

Escuela de Ciencias Químicas, Universidad Pedagógica y Tecnológica de Colombia, Avenida Central del Norte 39-115, Tunja, Colombia. E-mail: diana.becerra08@uptc.edu.co; juan.castillo06@uptc.edu.co

[**Left to right**]: **Juan-Carlos Castillo and Diana Becerra**

Juan-Carlos Castillo, born in Cali, Colombia, completed his undergraduate studies in Chemistry at the Universidad del Valle, where he also earned his PhD in Chemical Sciences in 2013 under the supervision of Prof. Rodrigo Abonía. From 2013 to 2015, he conducted postdoctoral research at the Institute des Sciences Moléculaires de Marseille in France, collaborating with Prof. Jean Rodríguez and Prof. Yoann Coquerel. Between 2015 to 2017, he served as a postdoctoral researcher at the Universidad de los Andes in Bogotá, Colombia, under the supervision of Prof. Jaime Portilla. In 2018, he began his academic career at the Universidad Pedagógica y Tecnológica de Colombia. His current research focuses on medicinal chemistry, supramolecular chemistry, and the application of catalysis in organic synthesis.

Diana Becerra, born in Florida, Colombia, completed her undergraduate studies in Chemistry at the Universidad del Valle in Cali, Colombia. She earned her PhD in Chemical Sciences in 2014 under the supervision of Prof. Braulio Insuasty. From 2014 to 2015, she conducted postdoctoral research at the Institut des Sciences Moléculaires de Marseille in France, working in collaboration with Prof. Jean Rodríguez and Prof. Damien Bonne. In 2017, she began her academic career at the Universidad Pedagógica y Tecnológica de Colombia. Her current research focuses on organic chemistry and medicinal chemistry.

1. Introduction

Pyrazole, a five-membered heterocycle with two adjacent nitrogen atoms, displays unique reactivity in organic chemistry: nucleophilic attacks are favored at positions 3 and 5, while electrophilic substitution reactions predominantly occur at position 4.[1] Within the azole family, pyrazole and its derivatives have attracted considerable attention due to their diverse applications across multiple fields, including medicine,[2,3] agriculture,[4] catalysis,[5] ion detection sensors,[6] supramolecular,[7] coordination,[8] and polymer chemistry,[9] as well as in the food,[10] cosmetic,[11] and petrochemical industries.[12] Notably, pyrazole derivatives are considered privileged scaffolds in drug discovery programs and medicinal chemistry due to their extensive range of pharmacological properties, such as antibacterial, antifungal, antioxidant, neuroprotective, anti-inflammatory, antimycobacterial, antimalarial, anticonvulsant, and antiviral activities, among others.[13–18] Several FDA-approved tyrosine kinase inhibitors (TKIs) incorporate a pyrazole scaffold, emphasizing its pivotal role in the development of effective cancer therapies. Examples include Crizotinib and Pralsetinib, both used for the treatment of non-small cell lung cancer (NSCLC),[19,20] Avapritinib, indicated for the management of multidrug-resistant gastrointestinal tumors,[21] and Asciminib and Rebastinib, which are employed in the treatment of chronic myeloid leukemia (Fig. 1).[22,23] Moreover, pyrazole derivatives have demonstrated multiple mechanisms of anticancer action by interacting with diverse targets such as tubulin,[2,24] epidermal growth factor receptor (EGFR),[25] cyclin-dependent kinase (CDK),[26] DNA,[27] topoisomerase,[28] and human carbonic anhydrase (hCA) IX.[29]

The extensive applications of pyrazole derivatives have driven the synthetic community to develop time-efficient and eco-friendly methodologies.[30–35] Among these, microwave-, ultrasound-, and mechanochemical-assisted synthesis have emerged as highly effective approaches for facilitating multiple bond formations under solvent-free conditions. These innovative methodologies not only reduce reaction times and temperatures but also achieve higher yields compared to conventional heating methods.[36–38] Such advancements constitute a significant contribution to the progress of sustainable chemistry, aligning closely with the fundamental principles of green chemistry.

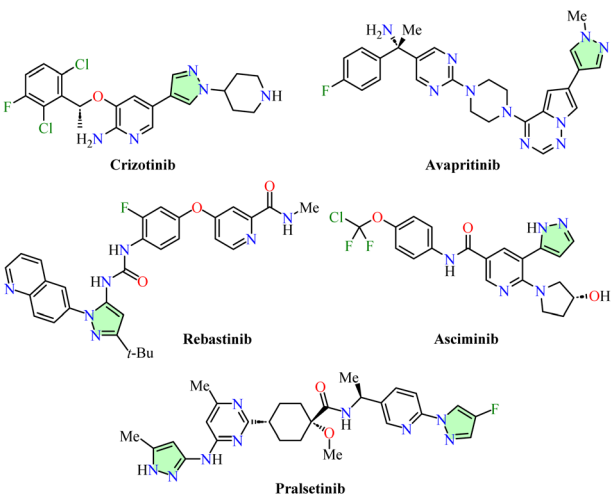

Fig. 1 FDA-approved pyrazole-based drugs for cancer treatment.

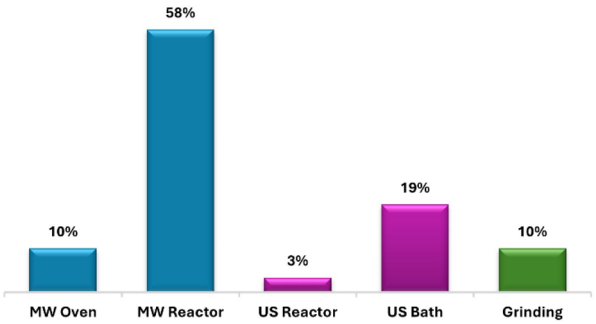

Fig. 2 Bibliometric graph illustrating the percentage of articles related to microwave-, ultrasound-, and mechanochemical-assisted synthesis of pyrazole derivatives with anticancer activity from 2014 to 2024 [data were collected from a Scopus search using the keywords: "pyrazole derivatives", "anticancer activity", "microwave", "ultrasound", and "mechanochemical"].

This review provides a comprehensive analysis of articles published from 2014 to 2024, focusing on the synthesis of pyrazole derivatives with anticancer activity using microwave, ultrasound, and mechanochemical techniques (Fig. 2). Notably, microwave irradiation was employed in 68% of the reviewed articles, employing both ovens and reactors, while 22% of studies relied on ultrasound irradiation, including baths and reactors, and 10% adopted mechanochemical approaches, primarily involving grinding with a mortar and pestle. Accordingly, the review is structured into three sections: the first explores the microwave-assisted synthesis of pyrazole derivatives, followed by sections examining ultrasound- and mechanochemical-assisted methods, each evaluating their respective anticancer efficacy.

2. Microwave-assisted synthesis of pyrazole derivatives

Microwave chemistry has transformed organic synthesis by introducing more sustainable protocols that overcome the limitations of conventional heating methods. Microwave-assisted organic synthesis (MAOS) enables the use of environmentally friendly solvents or even solvent-free conditions.[39] Selective dielectric heating drastically reduces reaction times and energy consumption, resulting in enhanced electivity and higher yields compared to traditional reflux-based processes.[40–42] Despite its advantages, MAOS has certain limitations, including (i) uneven heating, which may lead to localized overheating, side reactions, or thermal degradation, (ii) the requirement for specialized and costly reactors, which limits accessibility and presents challenges for industrial scalability, and (iii) poor microwave absorption in certain solvents, reducing heating efficiency and restricting its broader applicability.

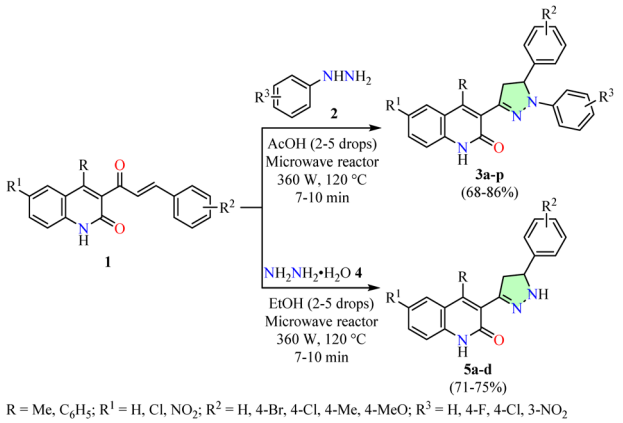

Scheme 1 Synthesis and anticancer evaluation of quinolin-2(1*H*)-one-based pyrazole derivatives **3** and **5**.

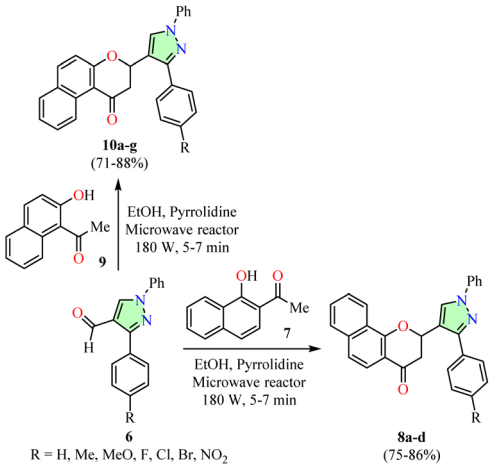

Scheme 2 Synthesis and anticancer evaluation of pyrazolyl-substituted benzochroman-4-ones **8** and **10**.

In this context, Sankaran *et al.* reported the microwave-assisted synthesis of quinolin-2(1*H*)-one-based pyrazole derivatives **3** in 68–86% yields *via* a reaction between quinolin-2(1*H*)-one-based α,β-unsaturated ketones **1** and arylhydrazines **2** in acetic acid using a microwave reactor set at 360 W and 120 °C for 7–10 min (Scheme 1).[43] Additionally, the protocol was extended to hydrazine hydrate **4** using ethanol under identical experimental conditions, affording quinolin-2(1*H*)-one-based pyrazoles **5** with yields ranging from 71% to 75%. This procedure is notable for its short reaction times, high yields, minimal solvent use, and broad substrate scope. Additionally, select compounds **3** and **5** were evaluated for anticancer activity against cervical (HeLa) and colon (HCT-116 and HCT-8) cancer cell lines using the 3-(4,5-dimethylthiazol-2-yl)-2,5-diphenyltetrazolium bromide (MTT) assay, with Adriamycin as the reference drug. Notably, compound **3i** (R = C_6H_5, R^1 = H, R^2 = 4-MeO, R^3 = H) exhibited the highest potency against HeLa cells, with an IC_{50} value of 2.4 ± 0.14 μM, making it 2.6-fold more potent than Adriamycin (IC_{50} = 6.3 ± 0.22 μM). Similarly, compound **3i** demonstrated 4.0-fold greater potency against HCT-116 cells (IC_{50} = 2.2 ± 0.12 μM) and 1.3-fold greater potency against HCT-8 cells (IC_{50} = 5.6 ± 0.16 μM) compared to Adriamycin (IC_{50} = 8.7 ± 0.20 μM and 7.2 ± 0.32 μM, respectively).

Ashok *et al.* reported the efficient synthesis of pyrazolyl-substituted benzochroman-4-ones **8** and **10** in good yields through the reaction of pyrazole 4-carbaldehydes **6** with acetylnaphthols **7** and **9**, respectively, in the presence of pyrrolidine and ethanol (Scheme 2).[44] The process was optimized using a microwave reactor set at 180 W for 5–7 min. Under reflux conditions, the same reaction resulted in lower yields (59–71%) and significantly longer reaction times (10–12 h). Moreover, compounds **8** and **10** were evaluated for their anticancer activity against breast (MCF-7), colon (Colo-205), and lung (A549) cancer cell lines using the MTT assay, with Adriamycin as the reference drug. Among them, compound **10b** (R = Me, GI_{50} < 0.1 μM) exhibited potency comparable to Adriamycin (GI_{50} = 0.13 μM) against MCF-7 cells. However, against Colo-205 and A549 cells, compound **10b** displayed GI_{50} values of 2.7 μM and 2.9 μM, respectively, indicating lower potency than Adriamycin (GI_{50} < 0.1 μM in both cell lines).

Desai *et al.* reported the Claisen–Schmidt condensation of 1-(1,3,4-oxadiazol-3(2*H*)-yl)ethan-1-one **11** with various aromatic aldehydes **12** in the presence of ethanolic potassium hydroxide using a microwave reactor at 400 W for 5–8 min, resulting in the formation of pyrazole-containing 1,3,4-oxadiazoles **13** in good yields (Scheme 3).[45] Conducting the same reaction under reflux conditions led to lower yields (59–66%) and longer reaction times (6–9 h). The mouse embryonic fibroblast cell line (NIH 3T3) and the cervical cancer cell line (HeLa) were used to assess the anticancer activity of compounds **13a–n**. However, data for the reference drug were not available. Among them, compounds **13a** (R = H) and **13d** (R = 3-Me) exhibited the highest potency against HeLa cells, with IC_{50} values of 58.47 μM and 56.60 μM, respectively, while displaying significantly lower potency against NIH 3T3 cells (IC_{50} > 100 μM).

The multicomponent reaction (MCR) strategy has proven highly effective in the pharmaceutical industry due to its high bond-forming efficiency and streamlined processes, enabling the rapid assembly of complex molecular architectures.[46,47] For example, Gomha *et al.* described a three-component reaction of 4-acetylpyrazole **14**, dimethylformamide dimethylacetal **15**, hydroximoyl chlorides **16**, and triethylamine in toluene using a microwave oven set at 150 °C and 500 W for 6 min, resulting in

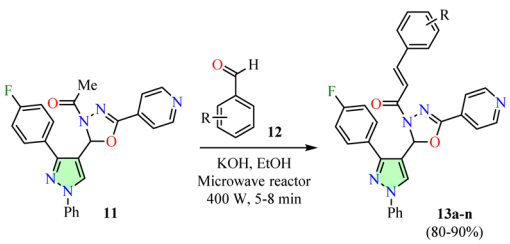

Scheme 3 Synthesis and anticancer evaluation of pyrazole-containing 1,3,4-oxadiazoles **13**.

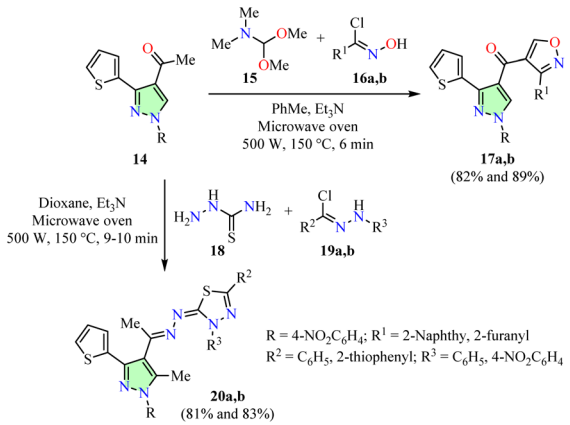

Scheme 4 Three-component synthesis and anticancer evaluation of pyrazole-based azoles **17** and **20**.

the formation of isoxazoles **17** in good yields (Scheme 4).[48] Moreover, a multicomponent reaction involving 4-acetylpyrazole **14**, thiosemicarbazide **18**, arylcarbohydrazonoyl chlorides **19**, and triethylamine in dioxane under similar microwave conditions led to the formation of 1,3,4-thiadiazoles **20** in good yields. Additionally, pyrazole-based azoles **17** and **20** were evaluated for their anticancer activity against lung (A549) and hepatocellular carcinoma (HepG2) cell lines using the MTT assay, with Cisplatin as the reference drug. Among them, compounds **17a** (R = 4-$NO_2C_6H_4$, R^1 = 2-naphthyl) and **17b** (R = 4-$NO_2C_6H_4$, R^1 = 2-furanyl) exhibited the highest potency against the A549 cell line with IC_{50} values of 4.47 ± 0.3 and 3.46 ± 0.6 μg mL^{-1}, making them 4.7- and 3.6-fold less potent than Cisplatin (IC_{50} = 0.95 ± 0.23 μg mL^{-1}). Similarly, compounds **17b** and **20b** (R = 4-$NO_2C_6H_4$, R^2 = R^3 = C_6H_5) demonstrated superior potency against the HepG2 cell line with IC_{50} values of 4.67 ± 0.9 and 5.67 ± 1.7 μg mL^{-1}, making them 3.3- and 4.1-fold less potent than Cisplatin (IC_{50} = 1.4 ± 0.37 μg mL^{-1}).

Arasakumar *et al.* reported the synthesis of 8-nitroquinoline derivatives **22** with good yields *via* a microwave-assisted reaction of arylhydrazines **2** with 3-arylidene-2,3-dihydro-8-nitro-4-quinolones **21** in ethanol using a microwave reactor set at 80 °C and 110 W for 7–10 min (Table 1).[49] The anticancer activity of compounds **22a–i** was evaluated against breast (MCF-7) and lung (A549) cell lines using the MTT assay, with Doxorubicin as the reference drug. Among them, compound **22g** (R = Cl, R^1 = 4-ClC_6H_4, R^2 = MeO) exhibited the highest potency against MCF-7 cells with an IC_{50} value of 25.76 μM, making it 1.7-fold less potent than Doxorubicin (IC_{50} = 15.12 μM). Similarly, compound **22b** (R = H, R^1 = 4-FC_6H_4, R^2 = H) showed the strongest activity against A549 cells with an IC_{50} value of 23.21 μM, making it 1.2-fold less potent than Doxorubicin (IC_{50} = 18.56 μM).

Subsequently, a molecular docking simulation was performed to analyze the interactions between compound **22g** and the tyrosine kinase domain of the epidermal growth factor receptor (EGFR) (PDB ID: 1M17) (Fig. 3).[49] The docking analysis revealed that the NH group in the tetrahydroquinoline ring forms a hydrogen bond with the ASN818 residue.

Table 1 Synthesis and anticancer evaluation of pyrazole derivatives **22**

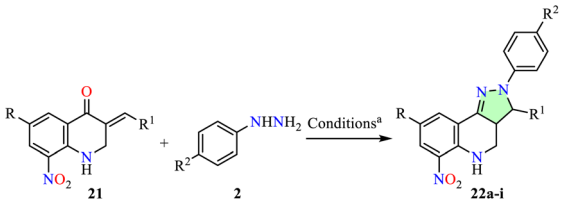

					IC_{50}[b] (μM)	
Compound	R	R^1	R^2	Yield **22**	MCF-7	A549
22a	H	C_6H_5	H	87	53.38	59.78
22b	H	4-FC_6H_4	H	90	45.98	23.21
22c	H	4-BrC_6H_4	H	89	34.72	29.57
22d	H	4-ClC_6H_4	H	89	41.35	28.66
22e	H	4-$MeOC_6H_4$	H	91	31.31	40.17
22f	H	4-MeC_6H_4	H	87	72.80	45.79
22g	Cl	4-ClC_6H_4	MeO	85	25.76	31.98
22h	H	3,4-$(MeO)_2C_6H_3$	H	83	58.54	46.36
22i	H	3,4-$(EtO)_2C_6H_3$	H	81	65.73	50.91
Doxorubicin	—	—	—	—	15.12	18.56

[a] Reaction conditions: arylhydrazines **2** and 3-arylidene-2,3-dihydro-8-nitro-4-quinolones **21** in EtOH using a microwave reactor set at 80 °C and 110 W for 7–10 min. [b] The half-maximal inhibitory concentration (IC_{50}) of each compound was determined by treating cells for 72 h, with untreated cells serving as controls. Cell viability was assessed using the MTT assay.

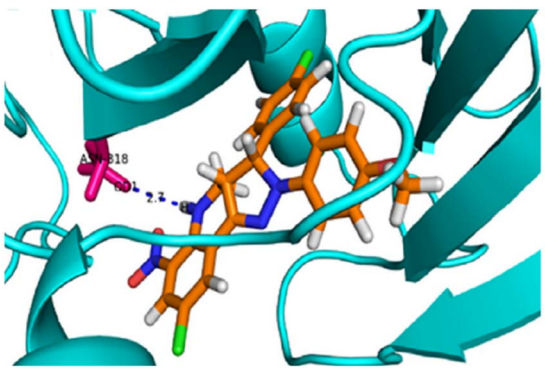

Fig. 3 3D representation of the interactions between compound **22g** and the epidermal growth factor receptor (EGFR) tyrosine kinase domain (PDB ID: 1M17). Reproduced with permission from ref. 49. Copyright Elsevier Inc., 2024.

Mótyán *et al.* reported an iodine-mediated oxidative cyclization of dihydrotestosterone (DHT) **23** with various arylhydrazines **2** in ethanol using a microwave reactor set at 100 °C for 2 min, resulting in the formation of DHT-derived pyrazoles **24** in 80–89% yields (Scheme 5).[50] This protocol is notable for its reduced reaction times and the elimination of the need to isolate pyrazoline intermediates. The anticancer activity of the synthesized compounds **24a–j** was evaluated against prostate (PC-3 and DU 145), breast (MCF-7 and MDA-MB-231), and cervical (HeLa) cancer cell lines, as well as non-cancerous MRC-5 fibroblasts, using the MTT assay. However, data for the

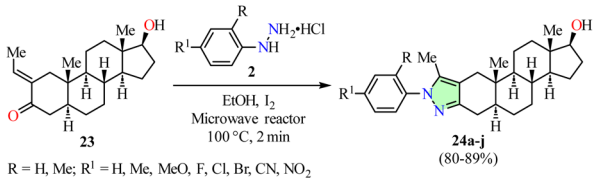

Scheme 5 Synthesis and anticancer evaluation of DHT-derived pyrazoles **24**.

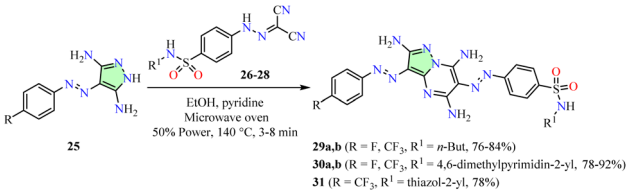

Scheme 6 Synthesis and anticancer evaluation of pyrazolo[1,5-*a*]pyrimidines **29–31**.

reference drug were not available. The IC_{50} values of compounds **24a–j** were consistently lower in all cancer cell lines compared to non-cancerous MRC-5 cells, suggesting a selective cytotoxic effect against malignant cells. Among them, compound **24e** (R = H, R^1 = MeO) exhibited the highest potency against PC-3 and DU 145 cells, with IC_{50} values of 4.2 ± 1.1 μM and 3.6 ± 1.2 μM, respectively. Similarly, compound **24e** showed the greatest potency against MCF-7 and MDA-MB-231 cells, with IC_{50} values of 5.5 ± 0.6 μM and 6.6 ± 0.9 μM, respectively, as well as against HeLa cells with an IC_{50} value of 8.5 ± 0.6 μM.

The effects of DHT-derived pyrazole **24e** on apoptosis and necrosis were evaluated in p53-deficient PC-3 cells, using cisplatin as a ref. 50. Treatment with **24e** significantly induced apoptosis, as evidenced by a high percentage of annexin V-positive cells (Q2 + Q3) at 33.96%, compared to less than 1% in the untreated control (Fig. 4a). Under the same experimental conditions, cisplatin also induced significant apoptosis. To further confirm apoptosis in PC-3 cells, quantitative real-time PCR revealed a significant increase in caspase 3 and Bax mRNA levels (Fig. 4b and c, respectively), indicating activation of the apoptotic pathway in both **24e** and cisplatin-treated PC-3 cells compared to the untreated control.

The remarkable biological and photophysical properties of functionalized pyrazolo[1,5-*a*]pyrimidines have generated increasing interest in their synthesis.[6,51] For instance, Fouda *et al.* reported a pyridine-catalyzed synthesis of pyrazolo[1,5-*a*]pyrimidines **29–31** in good yields *via* a cyclocondensation reaction of 3,5-diaminopyrazoles **25** with hydrazonoyl dicyanides **26–28** in ethanol using a microwave oven set at 50% power and 140 °C for 3–8 min (Scheme 6).[52] The anticancer activity of compounds **29–31** was evaluated against breast (MCF-7), hepatocellular carcinoma (HepG2), and colon (HCT-116) cancer cell lines using the MTT assay, with Doxorubicin as the reference drug. Among them, compound **31** (R = CF_3, R^1 = thiazol-2-yl) exhibited the greatest potency against MCF-7 cells with an IC_{50} value of 4.2 ± 0.2 μg mL^{-1}, which was 3.5-fold lower in potency compared to Doxorubicin (IC_{50} = 1.2 ± 0.2 μg mL^{-1}). Additionally, compound **30b** (R = CF_3, R^1 = 4,6-dimethylpyrimidin-2-yl) demonstrated the highest potency against HepG2 and HCT-116 cells, with IC_{50} values of 3.9 ± 0.4 μg mL^{-1} and 2.7 ± 0.6 μg mL^{-1}, respectively. However, it was 4.3- and 1.7-fold less potent than Doxorubicin (IC_{50} = 0.9 ± 0.3 μg mL^{-1} and 1.6 ± 0.2 μg mL^{-1}, respectively).

Shekarrao *et al.* reported an efficient palladium-catalyzed solvent-free synthesis of pyrazolo[1,5-*a*]pyrimidines **34** in good yields *via* the reaction of β-bromovinyl/aryl aldehydes **32** with 5-aminopyrazoles **33** using a microwave reactor set at 700 W and 120 °C for 15 min (Scheme 7).[53] The compounds **34a–k** were evaluated for their anticancer activity against cervical (HeLa) and prostate (DU-145) cell lines using the MTT assay, with Doxorubicin as the reference drug. Among them, compound **34d** exhibited the highest potency against HeLa and DU-145 cell lines, with IC_{50} values of 10.41 ± 0.217 μM and 10.77 ± 0.124 μM, respectively. However, it was 1.1- and 1.2-fold less potent than Doxorubicin, which exhibited IC_{50} values of 9.76 ± 0.114 μM and 9.00 ± 0.721 μM, respectively.

Aydın *et al.* reported the microwave-assisted synthesis of 1-aroyl-3,5-dimethyl-1*H*-pyrazoles **37** in 82–98% yields through a cyclocondensation reaction of carbohydrazide derivatives **35** with 2,4-pentanedione **36** in ethanol using a microwave oven set at 270 W for 3–5 min (Table 2).[54] The National Cancer Institute (NCI) evaluated the anticancer activity of compounds **37c**, **37d**, and **37f** across a panel of 60 human cancer cell lines using the Sulforhodamine B (SRB) assay at a concentration of 10 μM. However, data for the reference drug were not available. Interestingly, compound **37c** exhibited the highest growth inhibition percentage, achieving 69.95% against the K-562 leukemia cell line. Additionally, it demonstrated an IC_{50} value of 4.0 μM against the K-562 cell line, as determined by the MTT assay. Its

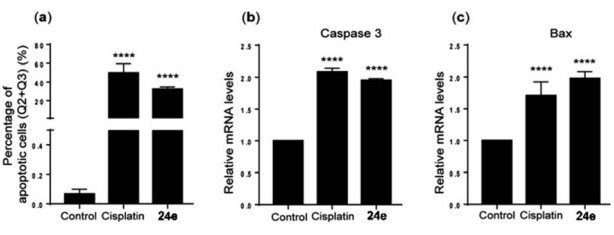

Fig. 4 (a) Quantification of apoptotic cells and relative mRNA expression levels of (b) caspase 3 and (c) Bax in PC-3 cells. Data are expressed as mean ± SD from three independent experiments. ****p < 0.0001 (Fisher's LSD test). This is an open-access article distributed under the terms of the Creative Commons CC BY license from ref. 50.

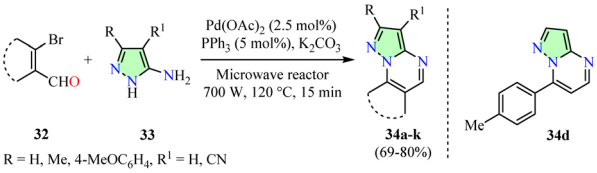

Scheme 7 Synthesis and anticancer evaluation of pyrazolo[1,5-*a*]pyrimidines **34**.

Table 2 Synthesis and anticancer evaluation of 1-aroyl-3,5-dimethyl-1*H*-pyrazoles **37**

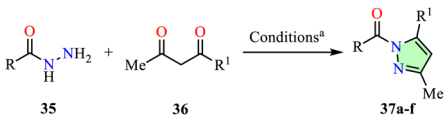

Compound	R	R^1	Yield 37
37a		Me	98
37b	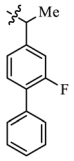	Me	97
37c	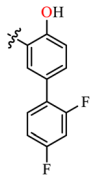	Me	86
37d	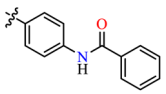	Me	82
37e	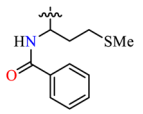	Me	82
37f	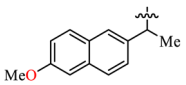	Me	98

[a] Reaction conditions: carbohydrazide derivatives **35** and 2,4-pentanedione **36** in ethanol using a microwave oven set at 270 W for 3–5 min.

apoptotic effects were further analyzed at concentrations of 1, 10, and 1000 μM over 24 h and 48 h, using TUNEL and Annexin V analyses. Notably, the addition of **37c** to K-562 cells induced apoptosis most effectively at a concentration of 10 μM, resulting in apoptosis rates of 12.0% and 22.5% after 24 h and 48 h, respectively.

Thalassitis *et al.* reported the one-pot synthesis of (2-pyrazolin-5-yl)methyl-9*H*-purines **40** in acceptable yields *via* a 1,3-dipolar cycloaddition reaction between 9-allyl-6-chloro-9*H*-purine **38** and nitrile imines, generated *in situ* from the corresponding hydrazones **39** in the presence of *N*-bromosuccinimide and triethylamine, using a microwave reactor set at 80 °C for 80 min (Scheme 8).[55] Interestingly, (pyrazol-5-yl)methyl-9*H*-purine **41** was obtained in 3% yield through the *in situ* oxidation of **40b** under microwave conditions. The National Cancer Institute (NCI) evaluated the anticancer activity of compounds **40** and **41** across a panel of 60 human cancer cell lines using the

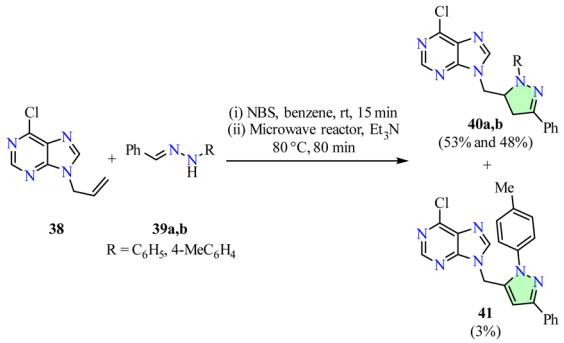

Scheme 8 Synthesis and anticancer evaluation of 9-substituted purines **40** and **41**.

SRB assay. However, data for the reference drug were not available. Notably, (pyrazol-5-yl)methyl-9*H*-purine **41** demonstrated the highest potency with GI_{50} values of 25.8, 36.1, and 36.8 μM against prostate (PC-3), renal (SN12C), and non-small cell lung (A549) cancer cell lines, respectively.

Reddy *et al.* reported an oxidative coupling reaction between various (hetero)aromatic aldehydes **12** and 4-amino-1-methyl-3-propyl-1*H*-pyrazole-5-carboxamide **42** using $K_2S_2O_8$ as the oxidizing agent in a DMSO : H_2O (1 : 1) mixture. The reaction was conducted in a microwave reactor set at 100 °C and 350 W for 3 min, resulting in the synthesis of 5-substituted-1*H*-pyrazolo[4,3-*d*]pyrimidin-7(6*H*)-ones **43** with yields ranging from 80% to 98% (Scheme 9).[56] The anticancer activity of compounds **43a–t** was evaluated against cervical (HeLa), renal (CAKI-I), prostate (PC-3), pancreatic (MiaPaCa-2), and lung (A549) cancer cell lines using the MTT assay. However, data for the reference drug were not available. Among them, compound **43m** (R = 3,5-$(MeO)_2C_6H_3$) exhibited the highest potency with IC_{50} values of 19 μM in HeLa cells, 17 μM in CAKI-I cells, 37 μM in PC-3 cells, 24 μM in MiaPaCa-2 cells, and 14 μM in A549 cells. Moreover, compound **43m** exhibited anticancer activity through an apoptotic mechanism and demonstrated mTOR inhibition with an IC_{50} value of 203 nM.

A molecular docking simulation was performed to analyze the interactions between compound **43m** and the active site of mTOR (PDB ID: 4JT5) (Fig. 5).[56] The results revealed that the oxygen atom of the C=O group in compound **43m** forms a hydrogen bond with the Val2240 residue, while the hydrophobic environment provided by Leu2185, Trp2239, Met2345,

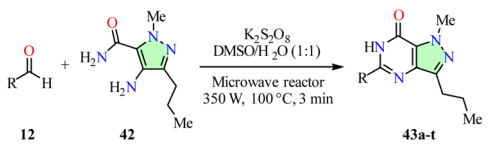

R = 2-EtOC6H4, 4-MeOC6H4, C6H5CH=CH, 3-Br-4-MeOC6H3, 3-NO2C6H4, 3-Br-4-FC6H3, 5-NO2-furan-2-yl, 4-HOC6H4, 4-ClC6H4, 2,4,5-(MeO)3C6H2, 3-NO2-4-MeOC6H3, 3-F-4-MeOC6H3, 3,5-(MeO)2C6H3, 3-ClC6H4, 2-FC6H4, 3-FC6H4, 3-NO2-4-OHC6H3, 3,4-(MeO)2C6H3, 3-pyridinyl, 3,4-(OCH2O)C6H3

Scheme 9 Synthesis and anticancer evaluation of 5-substituted-1*H*-pyrazolo[4,3-*d*]pyrimidin-7(6*H*)-ones **43**.

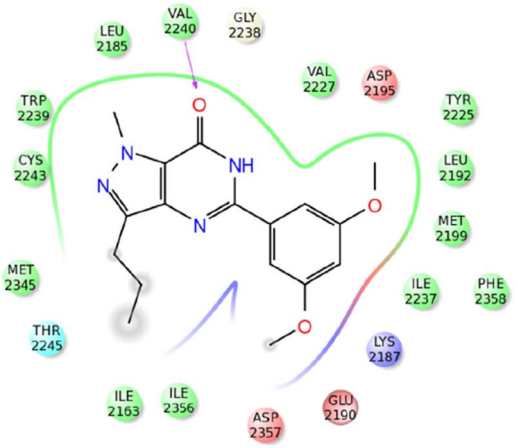

Fig. 5 2D representation of the interactions of compound **43m** with active site of mTOR (PDB ID: 4JT5). Reproduced with permission from ref. 56. Copyright Elsevier Inc., 2024.

and Ile2356 residues further enhances the stability of **43m** within the binding pocket.

Alnaja *et al.* reported the efficient synthesis of pyrazolo[1,5-*a*] pyrimidines **45** in 75–94% yields *via* a cyclocondensation reaction between 3,5-diaminopyrazoles **25** and β-enaminone **44** in acetic acid using a microwave reactor set at 110 °C and 800 W for 20–30 min (Scheme 10).[57] The anticancer activity of compounds **45a–g** was evaluated against colon (HCT-116), breast (MCF-7), and hepatocellular carcinoma (HepG2) cell lines using the MTT assay, with Doxorubicin as the reference drug. Among them, compound **45b** (R = 3-ClC_6H_4) exhibited the highest potency with IC_{50} values of 0.053 μM in HCT-116 cells, 0.126 μM in MCF-7 cells, and 0.039 μM in HepG2 cells, corresponding to 2.2-, 126.0-, and 19.5-fold lower potency, respectively, compared to Doxorubicin (IC_{50} = 0.024 μM, 0.001 μM, and 0.002 μM, respectively). The inhibitory activity of compound **45b** against CDK2/cyclin A3 was evaluated and compared to Lapatinib as the reference drug. Interestingly, Lapatinib (IC_{50} = 0.122 μM) exhibited 1.4-fold greater inhibitory activity than compound **45b** (IC_{50} = 0.178 μM).

A molecular docking simulation was performed to analyze the interactions between compound **45b** and the crystal structure of inhibitor B within the CDK2/A3 complex (PDB ID: 1H0V). The results revealed that the amino group of the pyrazolo[1,5-*a*] pyrimidine ring acted as a hydrogen bond donor to the carboxylic group of Asp86, while the nitrogen atom in the

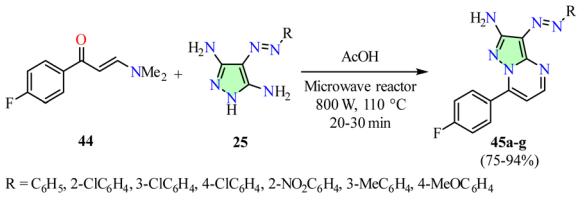

Scheme 10 Synthesis and anticancer evaluation of pyrazolo[1,5-*a*] pyrimidines **45**.

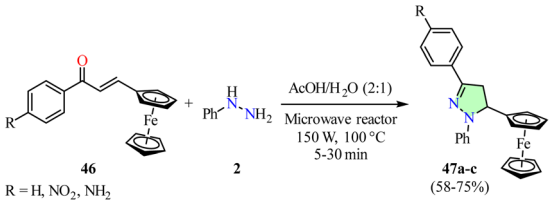

Scheme 11 Synthesis and anticancer evaluation of ferrocene-pyrazole hybrids **47**.

diazenyl moiety formed a strong hydrogen bond with the amino group of Lys89. Furthermore, the stability of compound **45b** within the binding pocket was enhanced by hydrophobic interactions, including two arene-H interactions between the pyrazolo[1,5-*a*]pyrimidine ring and the Ile10 and Val18 residues.[57]

Filho *et al.* reported the synthesis of ferrocene-pyrazole hybrids **47** in 58–75% yields *via* a cyclocondensation reaction between phenylhydrazine **2** and chalcones **46** in a mixture of acetic acid and water, using a microwave reactor set at 100 °C and 150 W for 5–30 min (Scheme 11).[58] The synthesized compounds **47a–c** were evaluated for anticancer activity against colon (HCT-116), prostate (PC-3), promyelocytic leukemia (HL60), and astrocytoma (SNB19) cancer cell lines using the MTT assay. However, data for the reference drug were not available. Notably, the ferrocene-pyrazole hybrid **47c** (R = NH_2) exhibited the highest anticancer activity with IC_{50} values of 3.12 μM in HCT-116 cells, 124.40 μM in PC-3 cells, 6.81 μM in HL60 cells, and 60.44 μM in SNB19 cells.

Molecular docking studies were performed to evaluate the interactions of compound **47c** with the tyrosine kinase domain of the epidermal growth factor receptor (EGFR) (PDB ID: 1M17) and the active site of the human IDH1 mutant (PDB ID: 5LGE) (Fig. 6a and b, respectively). The binding energies of compound **47c** with EGFR and IDH1 were determined to be −8.3 and −7.4 kcal mol^{-1}, respectively. Notably, the ferrocene moiety exhibited effective interactions within both the hydrophobic and hydrophilic cavities of these molecular targets.

Parikh *et al.* reported the one-pot multicomponent synthesis of pyrano[2,3-*c*]pyrazoles **50** under solvent-free conditions (Scheme 12).[59] Initially, a mixture of aryl hydrazine **2**, β-

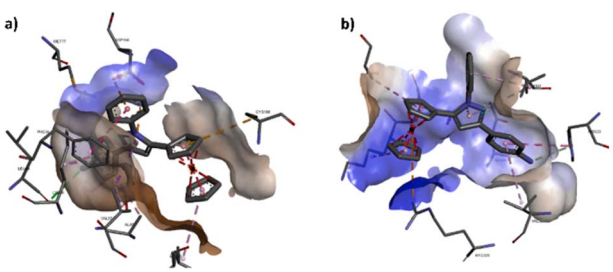

Fig. 6 3D representation of the interactions of compound **47c** with (a) the tyrosine kinase domain of the epidermal growth factor receptor (EGFR) (PDB ID: 1M17) and (b) the active site of the human IDH1 mutant (PDB ID: 5LGE). Reproduced with permission from ref. 58. Copyright Elsevier Inc., 2024.

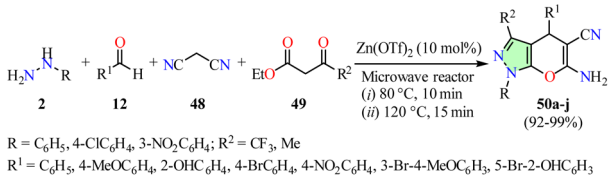

Scheme 12 Synthesis and anticancer evaluation of pyrano[2,3-*c*]pyrazoles **50**.

ketoesters **49**, and zinc triflate (10 mol%) was heated in a microwave reactor at 80 °C for 10 min. After cooling the reaction mixture to room temperature, aromatic aldehyde **12** and malononitrile **48** were added, and the mixture was further heated under microwave irradiation at 120 °C for 15 min. Recrystallization of the crude product in ethanol afforded pyrano[2,3-*c*]pyrazoles **50** in 92–99% yields. The synthesized compounds **50a–j** were evaluated for their anticancer activity against renal (786-0), epidermal (A431), breast (MCF-7), and glioblastoma (U-251) cancer cell lines using the MTT assay, with Doxorubicin as the reference drug. Among them, compound **50h** (R = 3-$NO_2C_6H_4$, R^1 = 4-$MeOC_6H_4$, R^2 = Me) exhibited the highest potency against the 786-0 and MCF-7 cell lines, with IC_{50} values of 9.9 ± 1.33 μg mL^{-1} and 31.87 ± 8.22 μg mL^{-1}, respectively. However, it was 10.0- and 15.2-fold less potent compared to Doxorubicin, which displayed IC_{50} values of 0.99 ± 0.17 μg mL^{-1} and 2.1 ± 0.79 μg mL^{-1}, respectively. Moreover, compound **50j** (R = 3-$NO_2C_6H_4$, R^1 = 5-Br-2-OHC_6H_3, R^2 = Me) exhibited the highest potency against the A-431 and U-251 cell lines, with IC_{50} values of 19.98 ± 6.01 μg mL^{-1} and 25.78 ± 8.47 μg mL^{-1}, respectively. However, it was 12.5- and 13.6-fold less potent compared to Doxorubicin, which displayed IC_{50} values of 1.6 ± 0.82 μg mL^{-1} and 1.9 ± 0.68 μg mL^{-1}, respectively.

Dahal *et al.* reported the synthesis of 1,3-diarylpyrazolones **51** in 66–93% yields through a cyclocondensation reaction between arylhydrazine hydrochlorides **2** and β-ketoesters **49** in a 1 : 1 mixture of water and glycerol, using a microwave reactor set at 100 °C and 300 W for 20 min (Table 3).[60] The anticancer activity of the synthesized compounds was evaluated against two human lung adenocarcinoma cell lines (A549 and NCI-H522) using the MTT assay, with Afatinib and Gefitinib as reference drugs. Interestingly, compound **51d** (R = C_6H_5, R^1 = H, R^2 = 4-ClC_6H_4) exhibited an IC_{50} value of 1.98 ± 1.10 μM against A549 cells, showing 4.3- and 7.2-fold greater potency compared to the clinically approved drugs Afatinib (IC_{50} = 8.46 ± 2.03 μM) and Gefitinib (IC_{50} = 14.27 ± 4.20 μM), respectively. Conversely, compound **51m** (R = R^2 = 4-BrC_6H_4, R^1 = H) displayed an IC_{50} value of 2.41 ± 0.57 μM against NCI-H522 cells, demonstrating 2.2- and 5.8-fold higher potency compared to Afatinib (IC_{50} = 5.34 ± 0.94 μM) and Gefitinib (IC_{50} = 13.86 ± 2.99 μM), respectively. In addition, the effect of compound **51j** (R = 4-$CF_3C_6H_4$, R^1 = H, R^2 = C_6H_5) on cell cycle progression in

Table 3 Synthesis and anticancer evaluation of 1,3-diarylpyrazolones **51**

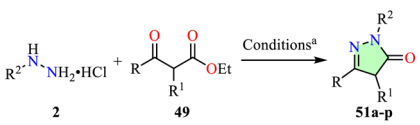

Compound	R	R^1	R^2	IC_{50}[b] (μM) A549	IC_{50}[b] (μM) NCI-H522
51a	Pr	H	C_6H_5	>100	>100
51b	C_6H_5	H	C_6H_5	10.35 ± 1.55	17.01 ± 2.61
51c	C_6H_5	H	4-BrC_6H_4	2.61 ± 1.12	4.93 ± 1.13
51d	C_6H_5	H	4-ClC_6H_4	1.98 ± 1.10	4.50 ± 1.16
51e	4-$NO_2C_6H_4$	H	C_6H_5	39.56 ± 1.05	40.5 ± 2.30
51f	4-BrC_6H_4	H	C_6H_5	6.35 ± 0.85	4.70 ± 1.38
51g	4-FC_6H_4	H	C_6H_5	9.51 ± 3.12	17.88 ± 3.36
51h	4-$MeOC_6H_4$	H	C_6H_5	42.25 ± 2.76	51.25 ± 3.06
51i	2-$MeOC_6H_4$	H	C_6H_5	>100	>100
51j	4-$CF_3C_6H_4$	H	C_6H_5	5.98 ± 0.84	4.88 ± 1.73
51k	2,3,4,5-$(F)_4C_6H$	H	C_6H_5	8.60 ± 0.59	9.9 ± 2.44
51l	4-FC_6H_4	H	4-BrC_6H_4	2.67 ± 0.51	3.70 ± 0.34
51m	4-BrC_6H_4	H	4-BrC_6H_4	2.73 ± 0.28	2.41 ± 0.57
51n	2-FC_6H_4	H	4-BrC_6H_4	3.58 ± 0.88	10.22 ± 1.30
51o	4-BrC_6H_4	H	4-$CF_3C_6H_4$	3.37 ± 0.10	2.95 ± 0.18
51p	4-BrC_6H_4	H	3,5-$(Cl)_2C_6H_3$	5.56 ± 0.07	5.07 ± 1.18
Afatinib	—	—	—	8.46 ± 2.03	5.34 ± 0.94
Gefitinib	—	—	—	14.27 ± 4.20	13.86 ± 2.99

[a] Reaction conditions: arylhydrazine hydrochlorides **2** and β-ketoesters **49** in a 1 : 1 mixture of water and glycerol using a microwave reactor set at 100 °C and 300 W for 20 min. [b] The half-maximal inhibitory concentration (IC_{50}) of each compound was determined by treating cells for 48 h with different doses ranging from 0 to 40 μM. Untreated cells served as controls, and cell viability was assessed using the MTT assay.

NCI-H522 cells was analyzed using flow cytometry. Treatment of NCI-H522 cells with compound **51j** at a concentration of 5 μM for 48 h resulted in a significant increase in the G_0/G_1 phase (72.73 ± 3.01%), while the S phase (11.23 ± 2.52%) and G_2/M phase (11.4 ± 1.10%) decreased accordingly.

The same research group evaluated the anticancer activity of 1,3-diarylpyrazolones **51a–p** against cutaneous melanoma (A375 and SKMEL-28) and non-melanoma skin cancer (A431 and SCC-12) cell lines using the MTT assay, with Celecoxib and Cisplatin as positive controls.[61] Among them, compound **51c** (R = C_6H_5, R^1 = H, R^2 = 4-BrC_6H_4) exhibited the highest potency against A375 and SKMEL-28 cells, with IC_{50} values of 14.3 ± 0.9 μM and 7.6 ± 0.6 μM, respectively. Compared to Celecoxib (IC_{50} = 26.8 ± 2.7 μM and 11.4 ± 2.4 μM, respectively), compound **51c** was 1.9- and 1.5-fold more potent. However, in comparison to Cisplatin (IC_{50} = 1.49 ± 0.44 μM and 14.2 ± 0.24 μM, respectively), it was 9.6-fold less potent in A375 cells but 1.9-fold more potent in SKMEL-28 cells. Similarly, compound **51c** exhibited the highest potency against A431 and SCC-12 cells, with IC_{50} values of 3.7 ± 0.5 μM and 12.2 ± 0.6 μM, respectively. Compared to Celecoxib (IC_{50} = 7.4 ± 0.6 μM and 44.1 ± 1.1 μM, respectively), compound **51c** was 2.0- and 3.6-fold more potent. However, in comparison to Cisplatin (IC_{50} = 7.7 ± 0.3 μM and 4.4 ± 0.2 μM, respectively), it was 2.1-fold more potent in A431 cells but 2.8-fold less potent in SCC-12 cells. Treatment of A431 and SK-MEL-28 cells with compound **51c** induced a pronounced, concentration-dependent induction of apoptosis, as evidenced by a significant increase in the levels of activated caspase-3, caspase-9, and cleaved PARP compared to untreated controls (Fig. 7).[61] These findings suggest that compound **51c** induces apoptosis in A431 and SKMEL-28 cells *via* the intrinsic mitochondrial apoptotic pathways, involving PARP activation.

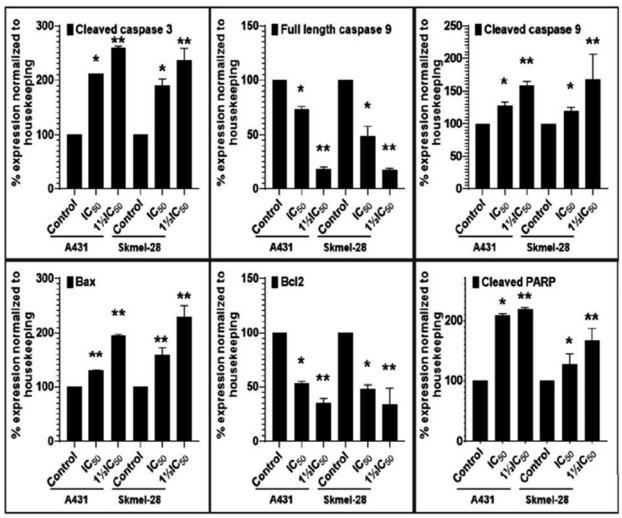

Fig. 7 Concentration-dependent effects (0, ½IC_{50}, IC_{50}, and 1½IC_{50}) of compound **51c** on the expression levels of apoptotic markers (caspase-3, caspase-9, Bax, Bcl2, and cleaved PARP) in SK-Mel-28 and A431 cancer cells after 48 h of treatment. β-actin was used as the loading control. Statistical significance was determined using Bonferroni's tests, with *p < 0.05 and **p < 0.01 considered significant. This is an open-access article distributed under the terms of the Creative Commons CC BY license from ref. 61.

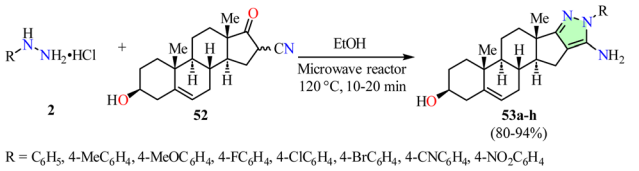

Scheme 13 Synthesis and anticancer evaluation of D-ring-fused steroidal 5-amino-1-arylpyrazoles **53**.

Mótyán *et al.* described the nucleophilic addition of the amine group from various arylhydrazines **2** to the carbonyl group of dehydroepiandrosterone derivatives **52** using a microwave reactor set at 120 °C for 10–20 min, resulting in the formation of D-ring-fused steroidal 5-amino-1-arylpyrazoles **53** with yields ranging from 80% to 94% (Scheme 13).[62] The anticancer activity of the synthesized compounds **53a–h** was evaluated against breast (MCF-7), prostate (PC-3), lung (A549), cervical (HeLa), and osteosarcoma (U2Os) cell lines using the MTT assay, with Cisplatin as the positive control. Among them, compound **53g** (R = 4-CNC_6H_4) exhibited the highest potency with IC_{50} values of 6.2 ± 1.0 μM in MCF-7 cells, 4.9 ± 1.1 μM in PC-3 cells, 7.9 ± 1.0 μM in A549 cells, and 4.0 ± 1.0 μM in HeLa cells, corresponding to approximately 54-, 184-, 47-, and 64-fold greater potency, respectively, compared to Cisplatin (IC_{50} = 338.5 ± 1.1 μM, 902 ± 1.6 μM, 369.8 ± 1.2 μM, and 254.5 ± 1.2 μM, respectively).

Ashok *et al.* reported a condensation reaction between 1-phenyl-1*H*-pyrazole-4-carbaldehydes **54** and *o*-phenylene diamine **55** in DMF using a microwave reactor set at 100 °C and 300 W for 7–9 min, resulting in the formation of pyrazole-based benzo[*d*]imidazoles **56** with yields ranging from 77% to 89% (Table 4).[63] The synthesized compounds **56a–g** were evaluated for their anticancer activity against brain (C6) and breast (MCF-7) cancer cell lines using the MTT assay, with Cisplatin as a positive control. Among them, compound **56b** (R = MeO) exhibited IC_{50} values of 0.102 μM and 0.110 μM against C6 and MCF-7 cells, respectively, demonstrating 1.2- and 5.4-fold higher potency compared to Cisplatin (IC_{50} = 0.122 μM and 0.596 μM, respectively).

Liao *et al.* reported the synthesis of 3,5-bis(styryl)pyrazoles **58** in acceptable yields through a cyclocondensation reaction of various curcuminoids **57** with hydrazine hydrate **4** in a 1 : 1 mixture of *N*,*N*-dimethylformamide and acetic acid, using a microwave reactor set at 80 °C for 5 min (Scheme 14).[64] The synthesized compounds **58a–l** were evaluated for their antiproliferative activity against the prostate cancer cell line (PC-3) using the MTT assay, with Methotrexate as the reference drug. Among them, compounds **58a** (R = R^3 = R^4 = H, R^1 = MeO, R^2 = OH) and **58l** (R = R^4 = Cl, R^1 = R^2 = R^3 = H) exhibited the highest potency against PC-3 cells with GI_{50} values of 0.85 ± 0.34 μM and 2.21 ± 0.33 μM, respectively. However, compounds **58a** and **58l** exhibited significantly lower potency than Methotrexate (GI_{50} = 0.012 ± 0.008 μM), being 71- and 184-fold less potent, respectively. Cell cycle analysis of PC-3 cells treated with

Table 4 Synthesis and anticancer evaluation of pyrazole-based benzo[*d*]imidazoles **56**

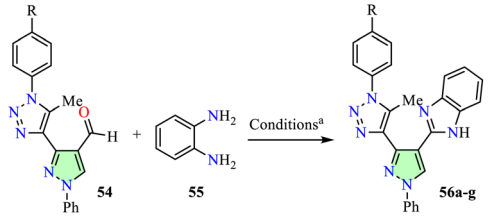

Compound	R	Yield	IC_{50}[b] (μM) C6	IC_{50}[b] (μM) MCF-7
56a	H	83	0.564	0.253
56b	MeO	84	0.102	0.110
56c	F	81	0.243	0.144
56d	Cl	89	3.220	0.185
56e	Br	87	0.219	0.450
56f	Me	85	0.120	0.303
56g	NO_2	77	0.560	0.452
Cisplatin	—	—	0.122	0.596

[a] Reaction conditions: 1-phenyl-1*H*-pyrazole-4-carbaldehydes **54** and *o*-phenylene diamine **55** in DMF using a microwave reactor set at 100 °C and 300 W for 7–9 min. [b] The half-maximal inhibitory concentration (IC_{50}) of each compound was determined by treating cells for 24 h with different doses (0.5, 0.25, 0.125, 0.0625, 0.0312, and 0.0156 mg mL^{-1}). Untreated cells served as controls, and cell viability was assessed using the MTT assay.

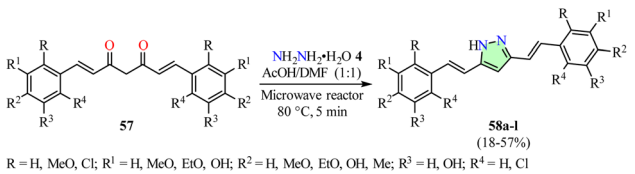

Scheme 14 Synthesis and anticancer evaluation of 3,5-bis(styryl)pyrazoles **58**.

bis(styryl)pyrazoles **58a** and **58l** for 72 h revealed a significant increase in the percentage of cells arrested in the G_2/M phase, reaching 89.6% and 89.3%, respectively. This G_2/M arrest inhibited cell division, leading to a reduced cell population in the G_0/G_1 phase (8.0% and 4.4%) and the *S* phase (2.2% and 6.3%). Furthermore, compound **58a** (K_d = 4.6 ± 1.1 μM) exhibited a 12-fold lower binding affinity for tubulin compared to compound **58l** (K_d = 0.4 ± 0.1 μM).

Molecular docking analysis was conducted to examine the interactions between compound **58l** and the tubulin-combretastatin A4 complex (PDB ID: 5LYJ). The binding energy of **58l** with tubulin was determined to be −8.4 kcal mol^{-1}. Remarkably, compound **58l** forms two hydrogen bonds within the paclitaxel binding site, interacting with the peptide backbone of residues T273 and P271 at distances of 2.2 Å and 2.6 Å, respectively (Fig. 8).[64]

Al-Wahaibi *et al.* reported a time-efficient microwave-assisted synthesis of 3,5-diaminopyrazole derivatives **60** in

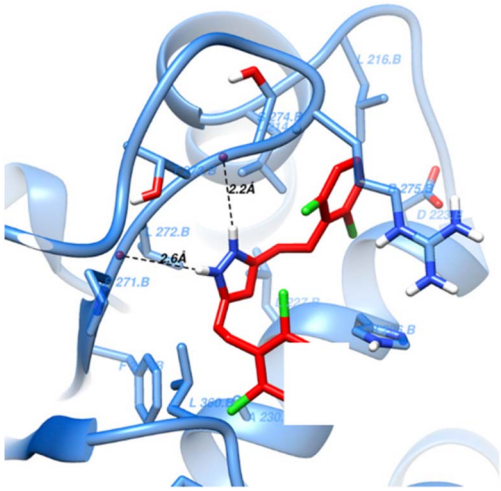

Fig. 8 3D representation of interactions between compound **58l** and the tubulin-combretastatin A4 complex (PDB ID: 5LYJ). This is an open-access article distributed under the terms of the Creative Commons CC BY license from ref. 64.

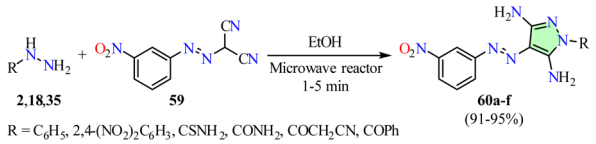

Scheme 15 Synthesis and anticancer evaluation of 3,5-diaminopyrazole derivatives **60**.

high yields through a cyclization reaction between arylhydrazines **2** and 2-((3-nitrophenyl)diazenyl)malononitrile **59** in ethanol (Scheme 15).[65] This method was successfully extended to thiosemicarbazide **18** and carbohydrazide derivatives **35** under similar reaction conditions. The synthesized compounds **60a–f** were evaluated for their anticancer activity against the breast cancer cell lines MCF-7 and MDA-MB-231 using the MTT assay, with Doxorubicin as the reference drug. Among them, compound **60a** (R = C_6H_5) exhibited an IC_{50} value of 6.20 ± 0.40 μM against MCF-7 cells, demonstrating 5.4-fold greater potency than Doxorubicin (IC_{50} = 33.20 ± 3.50 μM). Although compound **60c** (R = $CONH_2$) showed the highest activity against MDA-MB-231 cells with an IC_{50} value of 14.50 ± 1.10 μM, it was 4.5-fold less potent than Doxorubicin (IC_{50} = 3.20 ± 0.10 μM).

Sanad *et al.* reported the synthesis of pyrazole-linked pyrimidinones **62** in 72–85% yields through the reaction of 3-aryl-1*H*-pyrazol-5-amines **33** with thieno[2,3-*b*]pyridine-based enamines **61** in dioxane, using a microwave reactor set at 100 °C and 300 W for 30–45 min (Table 5).[66] The synthesized compounds **62a–e** were evaluated for their anticancer activity against breast (MCF-7), colon (Caco2), and liver (HEPG2) cancer cell lines using the MTT assay, with 5-fluorouracil (5-Fu) as the reference drug. Among them, compound **62c** (R = NO_2) exhibited IC_{50} values of 4.20 ± 0.33 μM in MCF-7 cells, 7.62 ± 0.51 μM in Caco2 cells, and 3.65 ± 0.29 in HEPG2 cells,

Table 5 Synthesis and anticancer evaluation of pyrazole-linked pyrimidinones **62**

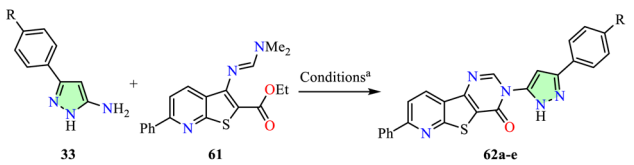

			IC_{50}[b] (μM)		
Compound	R	Yield	MCF-7	Caco2	HEPG2
62a	H	81	17.12 ± 1.38	23.93 ± 1.11	13.05 ± 0.72
62b	Cl	77	11.35 ± 0.92	13.38 ± 0.74	6.59 ± 0.48
62c	NO_2	72	4.20 ± 0.33	7.62 ± 0.51	3.65 ± 0.29
62d	Me	83	33.45 ± 1.25	44.72 ± 1.82	25.37 ± 0.97
62e	MeO	85	35.61 ± 1.85	47.55 ± 1.98	27.19 ± 1.15
5-FU	—	—	8.02 ± 0.77	12.20 ± 1.14	6.12 ± 0.52

[a] Reaction conditions: 3-aryl-1*H*-pyrazol-5-amines **33** and thieno[2,3-*b*]pyridine-based enamines **61** in dioxane using a microwave reactor set at 100 °C and 300 W for 30–45 min. [b] The half-maximal inhibitory concentration (IC_{50}) of each compound was determined by treating cells for 24 h with different doses (1, 2.5, 5, 10, 20, and 40 μg mL^{-1}). Untreated cells served as controls, and cell viability was assessed using the MTT assay.

demonstrating 1.9-, 1.6-, and 1.7-fold higher potency than 5-fluorouracil, respectively.

Molecular docking analysis was performed to investigate the interactions between compound **62c** and thymidylate synthase (PDB ID: 6QXG) (Fig. 9). The binding energy of **62c** with thymidylate synthase was determined to be −12.0 kcal mol^{-1}. Docking studies revealed hydrogen-bond interactions between the nitrogen atom and carbonyl oxygen of the pyrimidinone moiety with Arg215 and Tyr258, respectively. Additionally, compound **62c** formed hydrogen-bond interactions between the nitrogen atom of the pyrazole ring and Asp218, as well as between its nitro group and His196. Furthermore, a π–H stacking interaction was observed between the pyridine ring

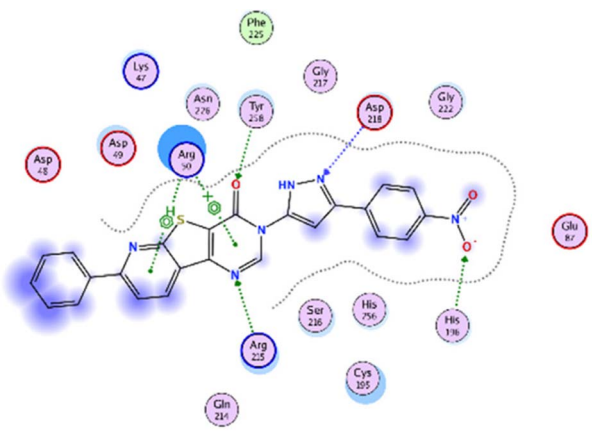

Fig. 9 2D representation of the interactions between compound **62c** and thymidylate synthase (PDB ID: 6QXG). Reproduced with permission from ref. 66. Copyright Elsevier Inc., 2024.

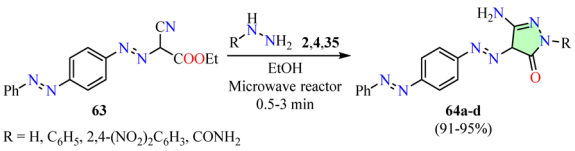

Scheme 16 Synthesis and anticancer evaluation of pyrazolone derivatives **64**.

and Arg50, along with a π–cation stacking interaction involving the pyrimidinone ring and Arg50.[66]

Anwer *et al.* reported a time-efficient synthesis of pyrazolone derivatives **64** in high yields through a cyclization reaction between arylhydrazines **2** and ethyl 2-cyano-2-{[4-(phenyldiazenyl)phenyl]diazenyl} acetate **63** in ethanol, using a microwave reactor for 0.5–3 min (Scheme 16).[67] This method was successfully extended to hydrazine hydrate **4** and carbohydrazide derivatives **35** under similar reaction conditions. The synthesized compounds **64a–d** were evaluated for their anticancer activity against liver (HEPG2), colon (HCT-116), breast (MCF-7), and lung (A549) cancer cell lines using the MTT assay, with Sorafenib and Erlotinib as reference drugs. Among them, compound **64b** (R = C_6H_5) exhibited the highest activity with IC_{50} values of 7.80 ± 0.70 μM in HEPG2 cells, 8.12 ± 0.90 μM in HCT-116 cells, 6.98 ± 1.10 μM in MCF-7 cells, and 6.50 ± 1.50 μM in A549 cells. However, it was 2.0-, 1.6-, 1.2-, and 1.6-fold less potent than Sorafenib, which exhibited IC_{50} values of 4.00 ± 0.33 μM, 5.05 ± 0.50 μM, 5.58 ± 0.55 μM, and 4.04 ± 0.33 μM, respectively. In contrast, compound **64b** exhibited comparable potency to Erlotinib (IC_{50} = 7.73 ± 0.67 μM, 13.91 ± 1.30 μM, 8.20 ± 0.34 μM, and 5.49 ± 0.45 μM, respectively) against HEPG2 and A549 cells, while exhibiting 1.7- and 1.2-fold greater potency against HCT-116 and MCF-7 cells, respectively. Moreover, compounds **64a–d** were further evaluated for their dual inhibitory effects on VEGFR-2 and $EGFRT^{790M}$. Among them, compound **64b** exhibited the strongest inhibition of VEGFR-2 with an IC_{50} value of 1.25 ± 0.50 μM, demonstrating 1.5-fold lower potency than Sorafenib (IC_{50} = 0.84 ± 0.04 μM). Additionally, compounds **64b** and **64c** (R = 2,4-$(NO_2)_2C_6H_3$) exhibited the highest inhibitory effects on $EGFRT^{790M}$ with IC_{50} values of 0.40 ± 0.35 μM and 0.35 ± 0.15 μM, respectively, showing 1.7- and 1.4-fold lower potency compared to Erlotinib (IC_{50} = 0.24 ± 0.22 μM).

3. Ultrasound-assisted synthesis of pyrazole derivatives

Ultrasound-assisted organic synthesis (UAOS) has become a crucial tool in sustainable chemistry, offering significant advantages over traditional methods. Its effectiveness is primarily attributed to the phenomenon of acoustic cavitation – the formation, growth, and implosive collapse of bubbles within a liquid medium – which generates localized high temperatures and pressures.[68,69] These "hot spots" greatly enhance chemical reactivity, facilitating a wide range of chemical transformations. UAOS enables reactions to proceed with

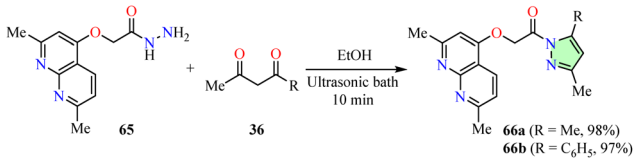

Scheme 17 Synthesis and anticancer evaluation of pyrazole-based 1,8-naphthyridines **66**.

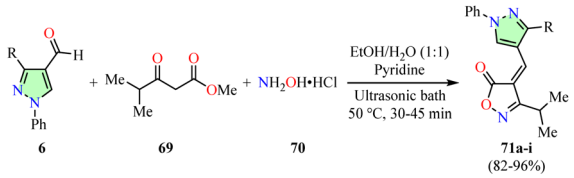

Scheme 19 Synthesis and anticancer evaluation of pyrazole-based isoxazol-5(4*H*)-ones **71**.

greater efficiency, achieving higher yields, and faster reaction rates at lower temperatures compared to conventional and microwave heating methods, thereby establishing itself as a cornerstone in the progress of sustainable chemistry.[70,71]

In this context, Ahmed *et al.* reported a cyclocondensation reaction of diketones **36** with 2-(2,7-dimethyl-1,8-naphthyridin-4-yloxy) acetohydrazide **65** in ethanol, using an ultrasonic bath for 10 min. This process resulted in the formation of pyrazole-based 1,8-naphthyridines **66a** and **66b** in 98% and 97% yields, respectively (Scheme 17).[72] The synthesized compounds **66a,b** were evaluated for their anticancer activity against the liver cancer cell line (HEPG2) using the MTT assay, with Doxorubicin as the reference drug. Among them, compounds **66a** (R = Me) and **66b** (R = C_6H_5) exhibited the highest potency against HEPG2 cells with IC_{50} values of 0.071 μM and 0.064 μM, respectively. However, compounds **66a** and **66b** exhibited lower potency than Doxorubicin (IC_{50} = 0.04 μM), making them 1.8- and 1.6-fold less potent, respectively.

Suresh *et al.* reported a three-component synthesis of pyrazolo[1,5-*a*]pyrimidines **68** in 37–88% yields through the reaction of 5-aminopyrazoles **33**, aromatic aldehydes **12**, and terminal alkynes **67** in acetic acid, using an ultrasonic bath set at 35 kHz and 60 °C for 30 min (Scheme 18).[73] To maintain a stable bath temperature of 60 °C during prolonged ultrasound irradiation, cold water was periodically added for temperature control. Selected compounds **68** were evaluated for their anticancer activity against breast cancer cell lines (MCF-7 and MDA-MB-231) using the SRB assay, with Gemcitabine as the reference drug. Inhibition percentages were recorded after 72 h of treatment with selected compounds **68** at a concentration of 10 μM. Among them, compound **68b** (R = CO_2Et, $R^1 = R^2$ = 4-MeC_6H_4) exhibited the highest inhibition percentage (25.12 ± 2.43%) against MCF-7 cells, being 2.0-fold more potent than Gemcitabine (49.56 ± 6.71%). Similarly, compound **68e** (R = CO_2Et, R^1 = C_6H_5, R^2 = 4-(*n*-Pent)C_6H_4) showed the highest inhibition percentage (62.16 ± 6.89%) against MDA-MB-231 cells, being 1.6-fold more potent than Gemcitabine (100.01 ± 1.13%).

Bhatt *et al.* described an efficient synthesis of pyrazole-based isoxazol-5(4*H*)-ones **71** in 82–96% yields through a three-component reaction involving 4-formylpyrazoles **6**, β-ketoester **69**, hydroxylamine hydrochloride **70**, and pyridine in a 1 : 1 ethanol–water mixture, using an ultrasonic bath set at 50 °C for 30–45 min (Scheme 19).[74] The National Cancer Institute (NCI) evaluated the anticancer activity of compounds **71a–i** across a panel of 60 human cancer cell lines using the SRB assay at a concentration of 10 μM. However, data for the reference drug were not available. Notably, compounds **71d** (R = 4-BrC_6H_4) and **71e** (R = 4-MeC_6H_4) exhibited the highest growth inhibition percentages, with values of −73.60% and −98.00%, respectively, against the LOX-IMVI melanoma cell line.

Nitulescu *et al.* reported the synthesis of pyrazole derivatives **73** in 67–77% yields through a one-pot reaction between 5-aminopyrazoles **33** and benzoyl isothiocyanates **72**, which were generated *in situ* from benzoyl chlorides and ammonium thiocyanate in acetonitrile, using an ultrasonic bath for 15–30 min (Scheme 20).[75] The anticancer activity of compounds **73a–f** was evaluated against colon (HT-29) and acute monocytic leukemia (THP-1) cell lines after 24 h of exposure at concentrations of 6.25, 12.5, 25, and 50 μg mL^{-1}, using the MTT assay. However, data for the reference drug were not available. THP-1 cells displayed greater sensitivity to the synthesized compounds than HT-29 cells. Notably, compound **73e** (R = Br, R^1 = Cl) exhibited an IC_{50} value of 40.34 μg mL^{-1}, while the other compounds showed IC_{50} values ranging from 42.97 μg mL^{-1} to 48.96 μg mL^{-1}. Apoptosis and necrosis were assessed in HT-29 cells treated with 50 μg mL^{-1} of compounds **73a–f** for 24 h using flow cytometry and the Annexin V-PI assay. Compound **73e** showed the highest necrosis-inducing effect, with 84.7% viable cells, 5.69% early apoptotic cells, 1.16% late apoptotic cells, and 8.43% necrotic cells. Furthermore, cell cycle analysis of HT-29 cells exposed to 50 μg mL^{-1} of compound **73e** for 24 h revealed a significant increase in the percentage of cells arrested

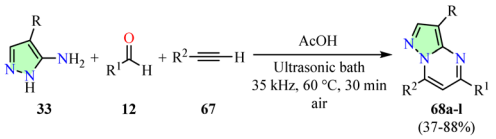

Scheme 18 Synthesis and anticancer evaluation of pyrazolo[1,5-*a*] pyrimidines **68**.

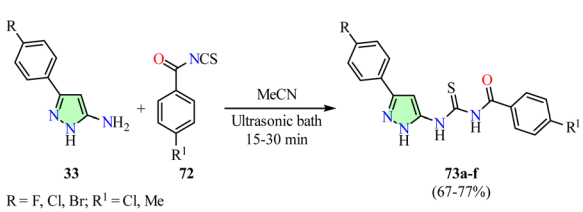

Scheme 20 Synthesis and anticancer evaluation of pyrazole derivatives **73**.

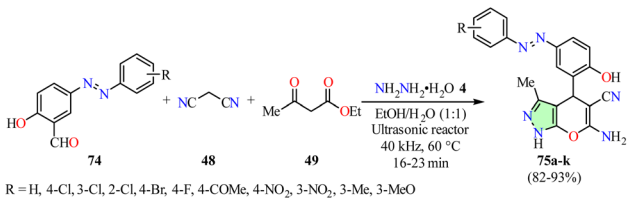

Scheme 21 Synthesis and anticancer evaluation of 1,4-dihydropyrano[2,3-c]pyrazole-5-carbonitriles **75**.

in the G_2/M phase (80.28%), leading to a reduced cell population in the G_0/G_1 (4.17%) and S (11.32%) phases compared to the control ($G_0/G_1 = 65.81\%$, $S = 22.49\%$, and $G_2/M = 10.03\%$). The G_2/M phase arrest induced by compound **73e** was associated with the upregulation of cyclin A, cyclin B, CDK1, and CDC20 gene expression.[75]

Nagasundaram *et al.* reported a catalyst-free synthesis of 1,4-dihydropyrano[2,3-*c*]pyrazole-5-carbonitriles **75** in 82–93% yields through a four-component reaction involving hydrazine hydrate **4**, malononitrile **48**, β-ketoester **49**, and arylazosalicylaldehydes **74** in a 1 : 1 ethanol–water mixture, using an ultrasonic reactor set at 40 kHz and 60 °C for 16–23 min (Scheme 21).[76] The anticancer activity of compounds **75h** (R = 4-NO_2) and **75i** (R = 3-NO_2) was evaluated against the HeLa cervical cancer cell line after 24 h of exposure at concentrations of 0.39, 0.78, 1.56, 3.12, 6.25, 12.5, 25, 50, and 100 μg mL^{-1}, using the MTT assay with Doxorubicin as the reference drug. Among them, compound **75i** exhibited the highest potency against HeLa cells with an IC_{50} value of 5.75 μg mL^{-1}, which is comparable to that of Doxorubicin (IC_{50} = 6.03 μg mL^{-1}).

Molecular docking analysis was performed to investigate the interactions between compound **75i** and the epidermal growth factor receptor (EGFR) tyrosine kinase domain (PDB ID: 1M17) (Fig. 10). The binding energy of **75i** with EGFR was determined to be −11.7 kcal mol^{-1}. Docking studies revealed seven hydrogen-bond interactions involving residues Lys721, Arg817, Asn818, Ala698, Asp813, and Gly833. Additionally, three electrostatic interactions were identified with Lys721, Glu738, and Asp831, along with one π–π stacking hydrophobic interaction with Phe699.[76]

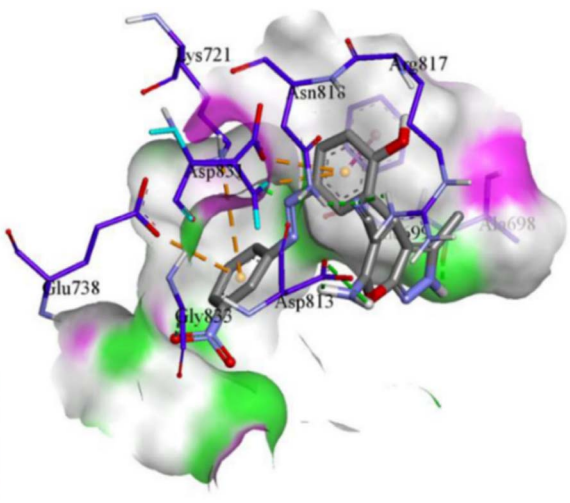

Fig. 10 3D representation of the interactions between compound **75i** and the epidermal growth factor receptor (EGFR) tyrosine kinase domain (PDB ID: 1M17). Reproduced with permission from ref. 76. Copyright Elsevier Inc., 2024.

Dofe *et al.* reported the synthesis of tetrazole-based pyrazole derivatives **77** in 93–98% yields through a cyclization reaction between hydrazine hydrate **4** and tetrazole-based chalcones **76** in ethanol, using an ultrasonic bath for 10–14 min (Table 6).[77] The compounds **77a–h** were evaluated for their anticancer activity against breast (MCF-7), lung (A549), and liver (HEPG2) cancer cell lines using the MTT assay, with Combretastatin A-4 (CA-4) as a positive control. Among them, compound **77c** (R = H, R^1 = F) exhibited the highest potency with IC_{50} values of 0.92 μM in MCF-7 cells, 0.94 μM in A549 cells, and 0.85 μM in HEPG2 cells. However, compound **77c** exhibited 23-, 19-, and 94-fold lower potency against MCF-7, A549, and HEPG2 cells, respectively, compared to Combretastatin A-4 (IC_{50} = 0.04 μM, 0.05 μM, and 0.009 μM, respectively). Moreover, compound **77c** displayed significant inhibition of tubulin polymerization (IC_{50} = 2.16 μM), being 1.3-fold less potent than Combretastatin A-4 (IC_{50} = 1.62 μM).

Molecular docking analysis was performed to investigate the interactions between compound **77c** and the colchicine binding site of α,β-tubulin (PDB ID: 1SA0) (Fig. 11). Docking studies revealed that the tetrazole ring aligns coplanarly with the Val238 residue, enabling it to act as a hydrogen bond donor. The 2-methoxy group on the central phenyl ring functions as a hydrogen bond acceptor for the thiol proton of Cys241.

Table 6 Synthesis and anticancer evaluation of tetrazole-based pyrazole derivatives **77**

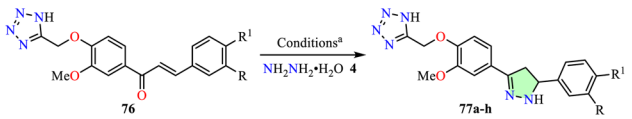

				IC_{50}[b] (μM)		
Compound	R	R^1	Yield	MCF-7	A549	HEPG2
77a	H	H	98	3.16	2.98	3.15
77b	H	Cl	97	1.04	1.11	0.96
77c	H	F	96	0.92	0.94	0.85
77d	MeO	MeO	95	2.94	2.82	3.06
77e	OH	H	96	2.16	2.24	2.88
77f	H	MeO	95	3.10	3.12	2.98
77g	H	Me	93	1.76	0.99	1.08
77h	H	OH	94	1.94	1.16	2.02
CA-4	—	—	—	0.04	0.05	0.009

[a] Reaction conditions: hydrazine hydrate **4** and tetrazole-based chalcones **76** in ethanol using an ultrasonic bath for 10–14 min. [b] The half-maximal inhibitory concentration (IC_{50}) of each compound was determined by treating cells for 72 h with different doses (200, 100, 50, 25, 12.5, 6.5, and 3.125 mg/100 μL). Untreated cells served as controls, and cell viability was assessed using the MTT assay.

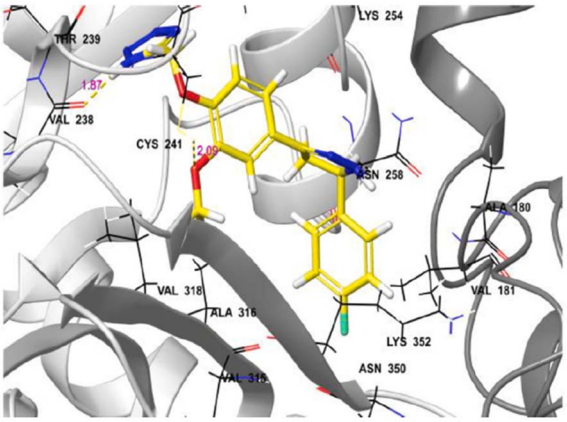

Fig. 11 3D representation of the interactions of compound **77c** with α,β-tubulin at the colchicine binding site (PDB ID: 1SA0). Reproduced with permission from ref. 77. Copyright Elsevier Inc., 2024.

Additionally, the pyrazoline and substituted phenyl groups are positioned within the hydrophobic pocket of tubulin, interacting with residues Asn258, Met259, Val315, Ala316, Val318, Asn350, Val351, and Lys352.[77]

Hassanin *et al.* reported the synthesis of carbazolyl–thiazolyl–pyrazole hybrids **79** in 88–92% yields through the cyclization of hydrazine hydrate **4** with carbazole–thiazolidinone–chromone hybrids **78** in ethanol, using an ultrasonic bath at 50 °C for 15 min (Table 7).[78] The anticancer activity of these compounds was evaluated against colon (HCT-116), prostate (PC-3), and liver (HEPG2) cancer cell lines using the SRB assay, with Doxorubicin as the reference drug. Among them, compound **79b** (R = allyl) exhibited the highest potency against HCT-116 and PC-3 cell lines, with IC_{50} values of 28.5 ± 1.5 μM and 4.9 ± 0.8 μM, respectively. Although compound **79b** was 4.1-fold less potent against HCT-116 cells, it exhibited 1.3-fold greater potency against PC-3 cells compared to Doxorubicin (IC_{50} = 6.9 ± 0.5 μM and 6.2 ± 0.9 μM, respectively). Additionally, compound **79e** (R = 4-ClC_6H_4) exhibited the highest anticancer activity against the HEPG2 cell line with an IC_{50} value of 9.1 ± 0.5 μM, making it 1.2-fold less potent than Doxorubicin (IC_{50} = 7.9 ± 1.3 μM).

Molecular docking analysis was performed to investigate the interactions between compound **79b** and the vascular endothelial growth factor receptor 2 (VEGFR2) kinase domain (PDB ID: 3EWH) (Fig. 12). The binding energy of **79b** with VEGFR2 was determined to be −11.2 kcal mol^{-1}. Docking studies revealed that the NH group of the pyrazole ring forms a hydrogen bond with Glu917, while the C=O group of the thiazole ring interacts with Thr916. Additionally, the thiazole ring engages in a π–cation interaction with Lys868, and the phenyl ring of the carbazole moiety participates in a π–anion interaction with Asp1046. Furthermore, π–alkyl interactions are observed between the carbazole or thiazole moieties and the residues Val848 and Leu889.[78]

4. Mechanochemical-assisted synthesis of pyrazole derivatives

Mechanochemistry utilizes mechanical energy generated through compression, shear, or friction to facilitate chemical transformations. This method is predominantly utilized under solvent-free conditions, offering notable advantages such as accelerated reaction rates, reduced reaction times, and enhanced control over product selectivity.[79,80] These benefits stem from the absence of solvation effects and the high reagent concentrations inherent to solvent-free systems.[79] Mechanochemical activation is typically achieved through three

Table 7 Synthesis and anticancer evaluation of carbazolyl–thiazolyl–pyrazole hybrids **79**

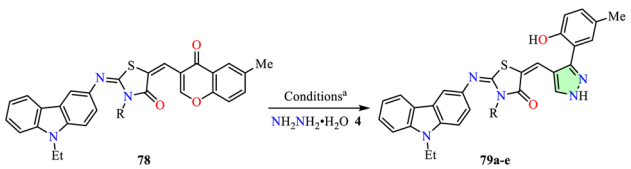

Compound	R	Yield	IC_{50}[b] (μM) HCT-116	PC-3	HEPG2
79a	Me	88	69.5 ± 1.5	12.9 ± 3.8	20.1 ± 0.2
79b	Allyl	88	28.5 ± 1.5	4.9 ± 0.8	18.5 ± 0.4
79c	Adamantan-1-yl	89	30.9 ± 2.3	37.4 ± 1.6	25.3 ± 1.4
79d	C_6H_5	92	>100	>100	>100
79e	4-ClC_6H_4	90	39.9 ± 0.1	9.2 ± 0.4	9.1 ± 0.5
Doxorubicin	—	—	6.9 ± 0.5	6.2 ± 0.9	7.9 ± 1.3

[a] Reaction conditions: hydrazine hydrate **4** and carbazole–thiazolidinone–chromone hybrids **78** in ethanol using an ultrasonic bath at 50 °C for 15 min. [b] The half-maximal inhibitory concentration (IC_{50}) of each compound was determined by treating cells for 72 h with different doses (0.01, 0.1, 1, 10, 100, and 1000 mg mL^{-1}). Untreated cells served as controls, and cell viability was assessed using the SRB assay.

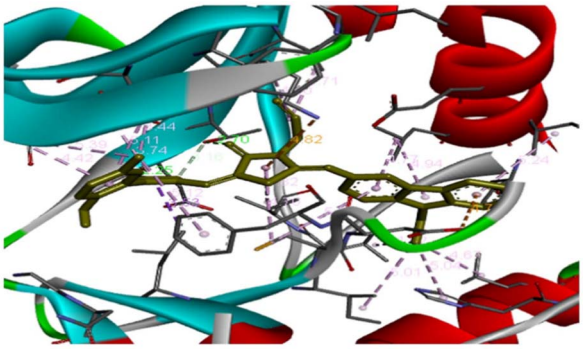

Fig. 12 3D representation of the interactions between compound **79b** and the vascular endothelial growth factor receptor 2 (VEGFR2) kinase domain (PDB ID: 3EWH). This is an open-access article distributed under the terms of the Creative Commons CC BY license from ref. 78.

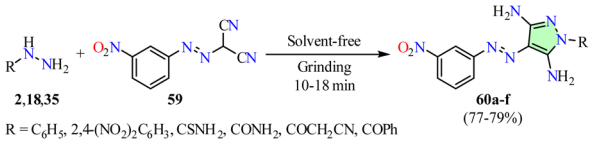

Scheme 22 Solventless synthesis of 3,5-diaminopyrazole derivatives **60**.

techniques: (a) grinding with a mortar and pestle, (b) planetary ball milling, and (c) high-speed vibration milling in a mixer mill.[81,82]

In this context, Al-Wahaibi *et al.* reported a solvent-free synthesis of 3,5-diaminopyrazole derivatives **60** in 77–79% yields by grinding arylhydrazines **2** with 2-((3-nitrophenyl)diazenyl)malononitrile **59** at room temperature for 10–18 min (Scheme 22).[65] This methodology was successfully extended to thiosemicarbazide **18** and carbohydrazide derivatives **35** under similar reaction conditions. The anticancer activity of compounds **60a–f** was previously discussed in the section on microwave-assisted synthesis of pyrazole derivatives (Scheme 15).

Rashdan *et al.* reported a solvent-free synthesis of pyrazolo[1,2-*b*]phthalazinediones **83** in 73–92% yields through a three-component reaction involving 1,2,3-triazolyl-pyrazolecarbaldehydes **80**, 6-nitrophthalhydrazide **81**, active methylene compounds such as malononitrile **48** or ethyl cyanoacetate **82**, and sodium hydroxide. The reaction was performed by grinding the components at room temperature for 20–30 min (Table 8).[83] The anticancer activity of these compounds was evaluated against HEPG2 liver cancer cells and BALAB/3T3 normal cells using the MTT assay, with Doxorubicin as the reference drug. Among them, compound **83f** (R = C_6H_5, R^1 = CO_2Et) exhibited the highest potency against the HEPG2 cell line with an IC_{50} value of 3.01 ± 0.21 μg mL^{-1}, making it 1.2-fold more potent than Doxorubicin (IC_{50} = 3.56 ± 0.46 μg mL^{-1}). Notably, compound **83f** showed no cytotoxicity toward the normal BALAB/3T3 cell line, demonstrating its selective anticancer activity.

Table 8 Synthesis and anticancer evaluation of pyrazolo[1,2-*b*] phthalazinediones **83**

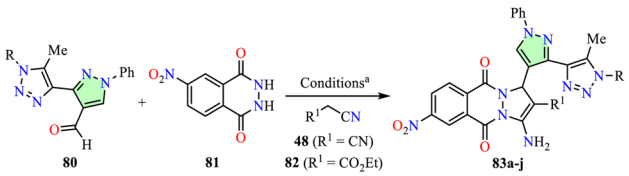

Compound	R	R^1	Yield	IC_{50}[b] (μg mL^{-1}) HEPG2	IC_{50}[b] (μg mL^{-1}) BALAB/3T3
83a	C_6H_5	CN	88	13.51 ± 4.48	18.24 ± 3.61
83b	4-ClC_6H_4	CN	82	ND	ND
83c	4-$MeOC_6H_4$	CN	73	22.73 ± 5.36	28.34 ± 7.61
83d	4-BrC_6H_4	CN	87	ND	ND
83e	4-$NO_2C_6H_4$	CN	86	ND	ND
83f	C_6H_5	CO_2Et	82	3.01 ± 0.21	ND
83g	4-ClC_6H_4	CO_2Et	82	ND	ND
83h	4-$MeOC_6H_4$	CO_2Et	82	ND	ND
83i	4-BrC_6H_4	CO_2Et	92	26.37 ± 6.17	30.04 ± 8.52
83j	4-$NO_2C_6H_4$	CO_2Et	91	ND	ND
Doxorubicin	—	—	—	3.56 ± 0.46	ND

[a] Reaction conditions: 1,2,3-triazolyl-pyrazolecarbaldehydes **80**, 6-nitrophthalhydrazide **81**, active methylene compounds **48** or **82**, and sodium hydroxide under grinding at room temperature for 20–30 min. [b] The half-maximal inhibitory concentration (IC_{50}) of each compound was determined by treating cells for 72 h with doses ranging from 0.1 to 100 μg mL^{-1}. Untreated cells served as controls, and cell viability was assessed using the MTT assay. ND: not detected at the concentrations tested.

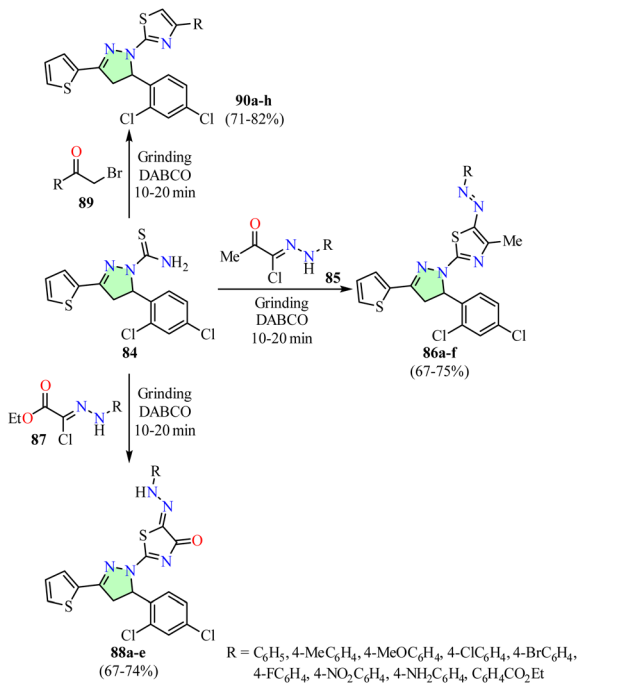

Scheme 23 Synthesis and anticancer evaluation of pyrazolylthiazoles **86**, **88**, and **90**.

Edrees *et al.* reported the cyclization of pyrazoline **84** with various hydrazonoyl chlorides **85** and **87** in the presence of 1,4-diazabicyclo[2.2.2]octane (DABCO), resulting in the formation of pyrazolylthiazoles **86** and **88** in 67–75% and 67–74%, respectively (Scheme 23).[84] Similarly, reacting α-bromoacetophenones **89** under identical conditions gave pyrazolylthiazoles **90** in 71–82% yields. In all cases, the reaction mixtures were ground for 10–20 min and subsequently poured into water. The resulting products were filtered and recrystallized from appropriate solvents to obtain the corresponding pyrazolylthiazoles. The anticancer activity of these compounds was evaluated against the HEPG2 liver cancer cell line using the MTT assay, with Cisplatin as the positive control. Among the tested compounds, pyrazolylthiazoles **90f** (R = 4-FC_6H_4) and **90d** (R = 4-ClC_6H_4) exhibited the highest potency against HEPG2 cells with IC_{50} values of 1.70 μM and 2.98 μM, respectively. However, compounds **90f** and **90d** were 1.9- and 3.3-fold less potent than Cisplatin (IC_{50} = 0.90 μM), respectively.

5. The structure activity relationship (SAR)

The biological activity of pyrazole derivatives is strongly influenced by the nature and position of substituents on the pyrazole core, as these modifications significantly affect their interactions with pharmacophoric targets, thereby modulating cytotoxicity and enzymatic inhibition. Structure–activity relationship (SAR) analysis demonstrates that specific substitutions at positions 1, 3, 4, and 5, along with structural fusions, are critical for enhancing anticancer activity. This enhancement is attributed to precise interactions with biological targets, including the induction of cell cycle arrest and the inhibition of key enzymes or proteins involved in cancer progression (Fig. 13). Moreover, Table 9 summarizes the structure–activity relationship (SAR) trends observed in this study, emphasizing the influence of specific substitutions on the pyrazole ring in anticancer activity. It highlights key substitution positions and molecular docking interactions with pharmacophoric targets. This comprehensive overview provides valuable insights into the structural features that contribute to enhanced anticancer activity.

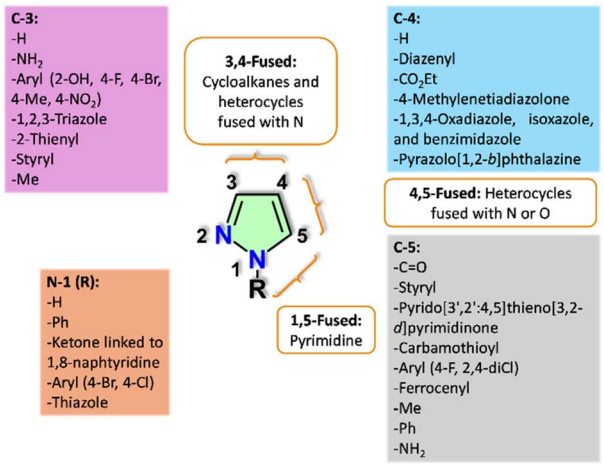

Fig. 13 SAR analysis of pyrazole derivatives with anticancer activity.

The aryl and heteroaryl substituents at position 1 play a crucial role in determining the binding affinity and biological activity of pyrazole derivatives. For instance, pyrazole derivatives substituted at position 1 with a ketone linked to 1,8-naphthyridine, aryl, or thiazole, in combination with 3,5-alkyl/aryl or hetaryl groups, exhibit significant biological activity. Docking studies have revealed strong interactions with the tyrosine kinase domain and the human IDH1 mutant, demonstrating potent activity against HEPG2 liver cancer cells, as confirmed by the MTT assay, with inhibitory effects that induce apoptosis and disrupt the cell cycle.[58,60,72,84] Additionally, substituents at positions 3 and 4, such as the 3-amino and 4-diazenyl groups, have demonstrated notable cytotoxic activity against MCF-7, HepG2, and HCT-116 cancer cell lines. These functional groups are essential for enhancing molecular interactions with cellular targets, thereby significantly improving cytotoxic efficacy.[52,57,67]

Pyrazolo[1,5-*a*]pyrimidine-fused derivatives substituted at positions 1 and 5 exhibit significant anticancer activity, particularly against MCF-7 and HCT-116 cell lines. The presence of an amino group at position 3 and a diazenyl group at position 4 enhances interactions with active sites, thereby improving anticancer efficacy.[52,53,57,73] Additionally, cyclofused derivatives at positions 3,4 and 4,5 containing cycloalkanes or nitrogen/oxygen-based heterocycles, have demonstrated notable activity against MCF-7 and HeLa cell lines. These derivatives inhibit key proteins involved in cancer progression, such as the epidermal growth factor receptor (EGFR) tyrosine kinase domain (*e.g.*, Lys721 and Asn818) and mTOR.[49,50,56,59,62,76]

In 1,3,4-substituted derivatives, the presence of 1-NH, 3-aryl, and 4-methylenetiadiazolone moieties facilitates strong docking interactions with the vascular endothelial growth factor receptor 2 (VEGFR2) kinase domain, further validating their anticancer activity.[78] Furthermore, 1,3,4-diaryl and hetaryl derivatives, including oxadiazole, isoxazole, and benzimidazole, exhibit broad-spectrum anticancer activity against HeLa, A549, MCF-7, LOX-IMVI, and HEPG2 cell lines, which can be attributed to their ability to form π–π interactions and hydrogen bonds with active site residues.[45,48,63,74,83]

At positions 1, 3, and 5, pyrazole and pyrazoline derivatives containing 1-NH, 3,5-bis(styryl), and 3-aryl/5-carbamothioyl substituents exhibit strong docking interactions with the tubulin-combretastatin A4 complex. These interactions disrupt microtubule polymerization, induce G_2/M phase arrest, and effectively inhibit cell division. Additionally, these derivatives interact with thymidylate synthase, forming hydrogen bonds with key residues such as Asp218, which enhance their activity against acute monocytic leukemia (THP-1).[64,66,75,77]

In 1,3,4,5-substituted derivatives, the presence of 1-aryl or $CONH_2$ groups, combined with 3,5-diamine and 4-diazenyl moieties, exhibits significant activity against MCF-7 and MDA-MB-231 cell lines. Their biological activity is attributed to interactions within key protein domains and mechanisms that induce G_2/M cell cycle arrest, effectively inhibiting cancer cell proliferation.[65]

Table 9 SAR analysis of pyrazole derivatives in anticancer activity

Substituted positions[a]	Key substitutions for enhanced activity	Compound	Anticancer activity or pharmacophoric interactions
3,4	3-Amine and 4-diazenyl groups	**30b**,[52] **31**,[52] **45b**,[57] **64b**[67]	Exhibits enhanced activity against MCF-7, HepG2, and/or HCT-116 cancer cell lines
1,5	Pyrimidine fusion in pyrazolo[1,5-*a*] pyrimidine with an amino group at position 3 and a diazenyl group at position 4 commonly observed	**30b**,[52] **31**,[52] **34d**,[53] **45b**,[57] **68b**,[73] **68e**[73]	Exhibits enhanced activity in MCF-7 and/or HCT-116 cancer cell lines
3,4 and 4,5	Fusion at positions 3,4 and 4,5 with cycloalkanes, as well as nitrogen- and oxygen-containing heterocycles	**22g**,[49] **24e**,[50] **43m**,[56] **50h**,[59] **53g**,[62] **75i**[76]	Exhibits enhanced activity against MCF-7 and HeLa cancer cell lines, with significant interactions observed in the epidermal growth factor receptor (EGFR) tyrosine kinase domain (PDB ID: 1M17) or through mTOR inhibition (PDB ID: 4JT5)
1,3,4	1-NH, 3-aryl, and 4-methylenetiadiazolone, with aryl groups containing OH and Me substitutions	**79b**[78]	Docking interactions with the vascular endothelial growth factor receptor 2 (VEGFR2) kinase domain (PDB ID: 3EWH)
1,3,4	1,3-Diaryl, 1-aryl-3-(2-tienyl), and 4-hetaryl (oxadiazole, isoxazole, and benzimidazole) groups directly attached to the pyrazole core or linked *via* methylene bridges	**13a**,[45] **13d**,[45] **17a**,[48] **17b**,[48] **56b**,[63] **71d**,[74] **71e**,[74] **83f**[83]	Enhances activity against Hela, A549, MCF-7, LOX-IMVI, and HEPG2 cancer cell lines
1,3,5	1-NH, 3,5-bis(styryl), 3,5-diaryl and 3-aryl-5-carbamothioyl moieties within a pyrazole or pyrazoline scaffold	**58a**,[64] **58l**,[64] **62c**,[66] **73e**,[75] **77c**[77]	Exhibits docking interactions with the tubulin-combretastatin A4 complex (PDB ID: 5LYJ) and the colchicine-binding site of α,β-tubulin (PDB ID: 1SA0), as well as interactions with thymidylate synthase (PDB ID: 6QXG). Additionally, it induces G2/M phase arrest in acute monocytic leukemia (THP-1) and PC-3 cancer cell lines
1,3,5	Substituted at position 1 with a ketone linked to 1,8-naphthyridine, an aryl, or a thiazole, while positions 3 and 5 are substituted with alkyl, aryl, or hetaryl groups, as well as ferrocene and carbonyl within a pyrazole or pyrazoline scaffold	**47c**,[58] **51c**,[60] **51d**,[60] **66a**,[72] **66b**,[72] **90d**,[84] **90f**[84]	Exhibits docking interactions with the tyrosine kinase domain (PDB ID: 1M17) and the human IDH1 mutant (R132H), along with significant activity against the HEPG2 liver cancer cell line
1,3,4,5	Substituted at position 1 with an aryl or amide group ($CONH_2$), along with 3,5-diamine and 4-diazenyl groups	**60a**,[65] **60c**[65]	Enhances activity against MCF-7 and MDA-MB-231 breast cancer cell lines

[a] The position numbers and types of substitutions on the pyrazole core are specified to categorize compounds with similar modifications, facilitating the SAR analysis of their effects on anticancer activity.

6. Conclusions and perspectives

This review highlights the diverse methodologies – microwave, ultrasound, and mechanochemical – employed in the synthesis of pyrazole derivatives with notable anticancer properties, emphasizing the strategic importance of these approaches in medicinal chemistry and drug discovery. The SAR analysis clearly demonstrates that targeted substitutions and structural modifications at positions 1, 3, 4, and 5 significantly enhance the anticancer activity of pyrazole derivatives by enabling precise interactions with key active site residues, including Lys721 (EGFR), Asn818 (EGFR), and Cys241 (tubulin), through hydrogen bonding, π–π interactions, and hydrophobic stabilization. These interactions drive critical mechanisms, including G_2/M phase arrest, apoptosis induction, and enzymatic inhibition, highlighting the potential of pyrazole derivatives as promising candidates for targeted anticancer therapies and future drug discovery initiatives.

Our analysis reveals that microwave irradiation is the most widely used method, representing 68% of the reviewed studies,

with reaction times ranging from 0.5 to 80 minutes and temperatures between 80 and 150 °C. Among microwave-assisted methodologies, dedicated microwave reactors are employed in 86% of cases, while conventional microwave ovens are employed in 14%. Ultrasound irradiation ranks as the second most applied technique, accounting for 22% of cases, with reaction times between 10 and 45 minutes and temperatures ranging from 50 to 60 °C. Within ultrasound-assisted methodologies, ultrasonic baths are utilized in 86% of cases, whereas ultrasonic reactors are applied in 14%. Mechanochemical activation is the least frequently employed method, representing 10% of cases, with reaction times ranging from 10 to 30 minutes at room temperature. Notably, all mechanochemical-assisted methodologies rely on grinding with a mortar and pestle. The integration of ultrasonic reactors and ball mills into the synthesis of anticancer pyrazole derivative presents significant potential for enhancing atom economy and step efficiency. Importantly, the lower market cost of ultrasonic reactors and ball mills compared to microwave reactors enables the development of more sustainable and cost-effective synthetic processes at reduced temperatures.

Data availability

No primary research results have been included and no new data were generated or analysed as part of this review.

Author contributions

The authors have made significant contributions to the development of this review, with no involvement from any other individuals. The specific contribution of each author are as follows: Dr Diana Becerra. Literature investigation, writing, manuscript review and editing, and conceptualization. Dr Juan-Carlos Castillo. Literature investigation, writing, manuscript review and editing, conceptualization, and supervision.

Conflicts of interest

There are no conflicts to declare.

Acknowledgements

J.-C. C. acknowledges the partial financial support provided by the Dirección de Investigaciones at the Universidad Pedagógica y Tecnológica de Colombia (Project SGI-3724). Additionally, D. B. and J.-C. C. express their sincere gratitude to Dr Irina Morales Castaño, Dean of the Facultad de Ciencias, and Dr Sandra Chaparro Acuña, Coordinator of the Doctorado en Ciencias Químicas, for their invaluable financial assistance.

Notes and references

1 J.-C. Castillo, B. Castro Agudelo, J. Gálvez, Y. Carissan, J. Rodríguez and Y. Coquerel, Periselectivity in the aza-Diels–Alder cycloaddition between α-oxoketenes and *N*-(5-pyrazolyl)imines: A combined experimental and theoretical study, *J. Org. Chem.*, 2020, **85**, 7368–7377.
2 Y. Zhang, C. Wu, N. Zhang, R. Fan, Y. Ye and J. Xu, Recent advances in the development of pyrazole derivatives as anticancer agents, *Int. J. Mol. Sci.*, 2023, **24**, 12724.
3 G. Li, Y. Cheng, C. Han, C. Song, N. Huang and Y. Du, Pyrazole-containing pharmaceuticals: Target, pharmacological activity, and their SAR studies, *RSC Med. Chem.*, 2022, **13**, 1300–1321.
4 Q. Fu, P.-P. Cai, L. Cheng, L.-K. Zhong, C.-X. Tan, Z.-H. Shen, L. Han, T.-M. Xu and X.-H. Liu, Synthesis and herbicidal activity of novel pyrazole aromatic ketone analogs as HPPD inhibitor, *Pest Manage. Sci.*, 2020, **76**, 868–879.
5 J.-C. Castillo, N.-F. Bravo, L.-V. Tamayo, P.-D. Mestizo, J. Hurtado, M. Macías and J. Portilla, Water-compatible synthesis of 1,2,3-triazoles under ultrasonic conditions by a Cu(I) complex-mediated click reaction, *ACS Omega*, 2020, **5**, 30148–30159.
6 A. Tigreros, J.-C. Castillo and J. Portilla, Cyanide chemosensors based on 3-dicyanovinylpyrazolo[1,5-*a*] pyrimidines: Effects of peripheral 4-anisyl group substitution on the photophysical properties, *Talanta*, 2020, **215**, 120905.
7 E. Moreno-Suárez, R. Avila-Acosta, K. Sánchez-Ramírez, J.-C. Castillo and M. A. Macías, Crystallographic, spectroscopic and thermal studies of 1-(4-bromophenyl)-5-(2,5-dimethyl-1*H*-pyrrol-1-yl)-3-methyl-1*H*-pyrazole, *Acta Crystallogr., Sect. C: Cryst. Struct. Commun.*, 2023, **79**, 472–479.
8 D. Fonseca, S. M. Leal-Pinto, M. V. Roa-Cordero, J. D. Vargas, E. M. Moreno-Moreno, M. A. Macías, L. Suescun, Á. Muñoz-Castro and J. J. Hurtado, Inhibition of *C. albicans* dimorphic switch by cobalt(II) complexes with ligands derived from pyrazoles and dinitrobenzoate: Synthesis, characterization and biological activity, *Int. J. Mol. Sci.*, 2019, **20**, 3237.
9 A. Kurt and M. Koca, Synthesis, characterization and thermal degradation kinetics of a new pyrazole derived methacrylate polymer, poly(1,3-diphenyl-1*H*-pyrazol-5-yl methacrylate), *Acta Chim. Slov.*, 2022, **69**, 466–477.
10 J. Zhang, W. Yang, M. He, Z. Peng and G. Wang, Development of novel pyrazole-1,2,4-triazole derivatives as tyrosinase inhibitors: Design, preparation, mechanism of action and anti-browning application, *Food Chem.*, 2024, **460**, 140722.
11 M. Guin, R. A. Roopa, P. Jain and N. B. Singh, Heterocyclic surfactants and their applications in cosmetics, *ChemistrySelect*, 2022, **7**, e202103989.
12 T.-F. Wang, S. R. Kosuru, S.-C. Yu, Y.-C. Chang, H.-Y. Lai, Y.-L. Chang, K.-H. Wu, S. Ding and H.-Y. Chen, Use of pyrazoles as ligands greatly enhances the catalytic activity of titanium *iso*-propoxide for the ring-opening polymerization of L-lactide: A cooperation effect, *RSC Adv.*, 2020, **10**, 40690–40696.
13 M. J. Naim, O. Alam, F. Nawaz, J. Alam and P. Alam, Current status of pyrazole and its biological activities, *J. Pharm. BioAllied Sci.*, 2016, **8**, 2–17.

14 B. Insuasty, A. Montoya, D. Becerra, J. Quiroga, R. Abonía, S. Robledo, I. D. Vélez, Y. Upegui, M. Nogueras and J. Cobo, Synthesis of novel analogs of 2-pyrazoline obtained from [(7-chloroquinolin-4-yl)amino]chalcones and hydrazine as potential antitumor and antimalarial agents, *Eur. J. Med. Chem.*, 2013, **67**, 252–262.

15 K. Karrouchi, S. Radi, Y. Ramli, Y. N. Mabkhot, J. Taoufik, F. A. Al-aizari and M. Ansar, Synthesis and pharmacological activities of pyrazole derivatives: A review, *Molecules*, 2018, **23**, 134.

16 M. Faisal, A. Saeed, S. Hussain, P. Dar and F. A. Larik, Recent developments in synthetic chemistry and biological activities of pyrazole derivatives, *J. Chem. Sci.*, 2019, **131**, 70.

17 O. Ebenezer, M. Shapi and J. A. Tuszynski, A review of the recent development in the synthesis and biological evaluations of pyrazole derivatives, *Biomedicines*, 2022, **10**, 1124.

18 D. Becerra, R. Abonía and J.-C. Castillo, Recent applications of the multicomponent synthesis for bioactive pyrazole derivatives, *Molecules*, 2022, **27**, 4723.

19 J. J. Cui, M. Tran-Dubé, H. Shen, M. Nambu, P.-P. Kung, M. Pairish, L. Jia, J. Meng, L. Funk, I. Botrous, M. McTigue, N. Grodsky, K. Ryan, E. Padrique, G. Alton, S. Timofeevski, S. Yamazaki, Q. Li, H. Zou, J. Christensen, B. Mroczkowski, S. Bender, R. S. Kania and M. P. Edwards, Structure based drug design of Crizotinib (PF-02341066), a potent and selective dual inhibitor of mesenchymal–epithelial transition factor (c-MET) kinase and anaplastic lymphoma Kinase (ALK), *J. Med. Chem.*, 2011, **54**, 6342–6363.

20 V. Subbiah, P. A. Cassier, S. Siena, E. Garralda, L. Paz-Ares, P. Garrido, E. Nadal, J. Vuky, G. Lopes, G. P. Kalemkerian, D. W. Bowles, M. Seetharam, J. Chang, H. Zhang, J. Green, A. Zalutskaya, M. Schuler, Y. Fan and G. Curigliano, Pan-cancer efficacy of pralsetinib in patients with RET fusion–positive solid tumors from the phase 1/2 ARROW trial, *Nat. Med.*, 2022, **28**, 1640–1645.

21 M. C. Heinrich, R. L. Jones, M. Mehren, P. Schöffski, C. Serrano, Y.-K. Kang, P. A. Cassier, O. Mir, F. Eskens, W. D. Tap, P. Rutkowski, P. S. P. Chawla, J. Trent, M. Tugnait, E. K. Evans, T. Lauz, T. Zhou, M. Roche, B. B. Wolf, S. Bauer and S. George, Avapritinib in advanced PDGFRA D842V-mutant gastrointestinal stromal tumour (NAVIGATOR): A multicentre, open-label, phase 1 trial, *Lancet Oncol.*, 2020, **21**, 935–946.

22 J. Schoepfer, W. Jahnke, G. Berellini, S. Buonamici, S. Cotesta, S. W. Cowan-Jacob, S. Dodd, P. Drueckes, D. Fabbro, T. Gabriel, J.-M. Groell, R. M. Grotzfeld, A. Q. Hassan, C. Henry, V. Iyer, D. Jones, F. Lombardo, A. Loo, P. W. Manley, X. Pellé, G. Rummel, B. Salem, M. Warmuth, A. A. Wylie, T. Zoller, A. L. Marzinzik and P. Furet, Discovery of asciminib (ABL001), an allosteric inhibitor of the tyrosine kinase activity of BCR-ABL1C, *J. Med. Chem.*, 2018, **61**, 8120–8135.

23 A. S. Harney, G. S. Karagiannis, J. Pignatelli, B. D. Smith, E. Kadioglu, S. C. Wise, M. M. Hood, M. D. Kaufman, C. B. Leary, W.-P. Lu, G. Al-Ani, X. Chen, D. Entenberg, M. H. Oktay, Y. Wang, L. Chun, M. Palma, J. G. Jones, D. L. Flynn and J. S. Condeelis, The selective Tie2 inhibitor rebastinib blocks recruitment and function of Tie2Hi macrophages in breast cancer and pancreatic neuroendocrine tumors, *Mol. Cancer Ther.*, 2017, **16**, 2486–2501.

24 M. A. Alam, Pyrazole: An emerging privileged scaffold in drug discovery, *Future Med. Chem.*, 2023, **15**, 2011–2023.

25 A. A. Gaber, A. M. El-Morsy, F. F. Sherbiny, A. H. Bayoumi, K. M. El-Gamal, K. El-Adl, A. A. Al-Karmalawy, R. R. Ezz Eldin, M. A. Saleh and H. S. Abulkhair, Pharmacophore-linked pyrazolo[3,4-*d*]pyrimidines as EGFR-TK inhibitors: Synthesis, anticancer evaluation, pharmacokinetics, and in silico mechanistic studies, *Arch. Pharm.*, 2021, e2100258.

26 M. F. Harras and R. Sabour, Design, synthesis and biological evaluation of novel 1,3,4-trisubstituted pyrazole derivatives as potential chemotherapeutic agents for hepatocellular carcinoma, *Bioorg. Chem.*, 2018, **78**, 149–157.

27 R. P. Paitandi, V. Sharma, V. D. Singh, B. K. Dwivedi, S. M. Mobin and D. S. Pandey, Pyrazole appended quinoline-BODIPY based arene ruthenium complexes: Their anticancer activity and potential applications in cellular imaging, *Dalton Trans.*, 2018, **47**, 17500–17514.

28 L. Gomez, M. D. Kack, J. Wu, J. J. M. Wiener, H. Venkatesan, A. Santillán, D. J. Pippel, N. Mani, B. J. Morrow, S. T. Motley, K. J. Shaw, R. Wolin, C. A. Grice and T. K. Jones, Novel pyrazole derivatives as potent inhibitors of type II topoisomerases. Part 1: Synthesis and preliminary SAR analysis, *Bioorg. Med. Chem. Lett.*, 2007, **17**, 2723–2727.

29 C. Yamali, H. I. Gul, A. Ece, S. Bua, A. Angeli, H. Sakagami, E. Sahin and C. T. Supuran, Synthesis, biological evaluation and in silico modelling studies of 1,3,5-trisubstituted pyrazoles carrying benzenesulfonamide as potential anticancer agents and selective cancer-associated hCA IX isoenzyme inhibitors, *Bioorg. Chem.*, 2019, **92**, 103222.

30 J. Zhou, Q. Zhou and J.-P. Wan, Recent advances in the multicomponent synthesis of pyrazoles, *Org. Biomol. Chem.*, 2024, **22**, 8065–8077.

31 S. Sharma, P. Sharma, B. Budhalakoti, A. Kumar, K. Singh, R. K. Kamboj and K. Bhatrola, Exploring the impact of ionic liquids on pyrazole derivatives synthesis: A critical review, *ChemistrySelect*, 2024, **9**, e202401925.

32 S. Sharma, V. Singh, Vaishali, R. Kumar, R. Jamra, N. Banyal and Jyoti, From 2011 to 2022: The development of pyrazole derivatives through the α,β-unsaturated carbonyl compounds, *J. Heterocycl. Chem.*, 2024, **61**, 232–284.

33 R. Singh, R. Kaur, P. Ahlawat, P. Kaushik and K. Singh, Green methods for the synthesis of pyrazoles: A review, *Org. Prep. Proced. Int.*, 2021, **53**, 317–351.

34 S. P. Chandrasekharan, A. Dhami, S. Kumar and K. Mohanan, Recent advances in pyrazole synthesis employing diazo compounds and synthetic analogues, *Org. Biomol. Chem.*, 2022, **20**, 8787–8817.

35 P. K. Mykhailiuk, Fluorinated pyrazoles: From synthesis to applications, *Chem. Rev.*, 2021, **121**, 1670–1715.

36 B. Nehra, V. Chawla, P. A. Chawla and M. Kumar, Recent advancements in microwave assisted synthesis of pyrazole

analogues: An ecological synthetic approach, *Polycyclic Aromat. Compd.*, 2024, **2024**, 1–47.
37 F. Tok and B. Koçyiğit-Kaymakçıoğlu, Recent advances in the microwave and ultrasound-assisted synthesis of pyrazole scaffolds, *Curr. Org. Chem.*, 2023, **27**, 1053–1071.
38 S. Singh, S. Yadav, M. Minakshi and R. Pundeer, Green synthesis of pyrazoles: Recent developments in aqueous methods, *SynOpen*, 2023, **7**, 297–312.
39 D. Dallinger and C. O. Kappe, Microwave-assisted synthesis in water as solvent, *Chem. Rev.*, 2007, **107**, 2563–2591.
40 A. Hoz, Á. Díaz-Ortiz and A. Moreno, Microwaves in organic synthesis. Thermal and non-thermal microwave effects, *Chem. Soc. Rev.*, 2005, **34**, 164–178.
41 C. O. Kappe, Microwave dielectric heating in synthetic organic chemistry, *Chem. Soc. Rev.*, 2008, **37**, 1127–1139.
42 K. Martina, G. Cravotto and R. S. Varma, Impact of microwaves on organic synthesis and strategies toward flow processes and scaling, *J. Org. Chem.*, 2021, **86**, 13857–13872.
43 M. Sankaran, C. Uvarani, K. Chandraprakash, M. U. Maheswari and P. S. Mohan, An expedient approach for the synthesis of bioactive pyrazole, isoxazole and benzodiazepine-substituted quinolin-2(1*H*)-one derivatives, *J. Heterocycl. Chem.*, 2015, **52**, 1082–1092.
44 D. Ashok, K. Padmavati, B. V. Lakshmi and M. Sarasija, Microwave-assisted one-pot synthesis of pyrazolyl-substituted benzochroman-4-one derivatives and evaluation of their anticancer activity, *Chem. Heterocycl. Compd.*, 2016, **52**, 15–20.
45 N. C. Desai, G. M. Kotadiya, A. R. Trivedi, V. M. Khedkar and P. C. Jha, Design, synthesis, and biological evaluation of novel fluorinated pyrazole encompassing pyridyl 1,3,4-oxadiazole motifs, *Med. Chem. Res.*, 2016, **25**, 2698–2717.
46 D. Insuasty, J. Castillo, D. Becerra, H. Rojas and R. Abonía, Synthesis of biologically active molecules through multicomponent reactions, *Molecules*, 2020, **25**, 505.
47 D. Hurtado-Rodríguez, A. Salinas-Torres, H. Rojas, D. Becerra and J.-C. Castillo, Bioactive 2-pyridone-containing heterocycle syntheses using multicomponent reactions, *RSC Adv.*, 2022, **12**, 35158–35176.
48 S. M. Gomha, M. M. Edrees, R. A. M. Faty, Z. A. Muhammad and Y. N. Mabkhot, Microwave-assisted one-pot three-component synthesis of some novel pyrazole scaffolds as potent anticancer agents, *Chem. Cent. J.*, 2017, **11**, 37.
49 T. Arasakumar, S. Mathusalini, S. Gopalan, S. Shyamsivappan, A. Ata and P. S. Mohan, Biologically active perspective synthesis of heteroannulated 8-nitroquinolines with green chemistry approach, *Bioorg. Med. Chem. Lett.*, 2017, **27**, 1538–1546.
50 G. Mótyán, M. K. Gopisetty, R. E. Kiss-Faludy, A. Kulmány, I. Zupkó, É. Frank and M. Kiricsi, Anti-cancer activity of novel dihydrotestosterone-derived ring A-condensed pyrazoles on androgen non-responsive prostate cancer cell lines, *Int. J. Mol. Sci.*, 2019, **20**, 2170.
51 A. Ballesteros-Casallas, M. Paulino, P. Vidossich, C. Melo, E. Jiménez, J.-C. Castillo, J. Portilla and G. Pietro Miscione, Synthesis of 2,7-diarylpyrazolo[1,5-*a*]pyrimidine derivatives with antitumor activity. Theoretical identification of targets, *Eur. J. Med. Chem. Rep.*, 2022, **4**, 100028.
52 A. M. Fouda, H.-A. S. Abbas, E. H. Ahmed, A. A. Shati, M. Y. Alfaifi and S. E. I. Elbehairi, Synthesis, *in vitro* antimicrobial and cytotoxic activities of some new pyrazolo[1,5-*a*]pyrimidine derivatives, *Molecules*, 2019, **24**, 1080.
53 K. Shekarrao, P. P. Kaishap, V. Saddanapu, A. Addlagatta, S. Gogoi and R. C. Boruah, Microwave-assisted palladium mediated efficient synthesis of pyrazolo[3,4-*b*]pyridines, pyrazolo[3,4-*b*]quinolines, pyrazolo[1,5-*a*]pyrimidines and pyrazolo[1,5-*a*]quinazolines, *RSC Adv.*, 2014, **4**, 24001.
54 S. Aydın, N. Kaushik-Basu, S. Özba-Turan, J. Akbuga, P. Mega Tiber, O. Orun, K. R. Gurukumar, A. Basu and G. Küçükgüzel, Synthesis of 1-aroyl-3,5-dimethyl-1*H*-pyrazoles as anti-HCV and anticancer agents, *Lett. Drug Des. Discovery*, 2014, **11**, 121–131.
55 A. Thalassitis, A.-M. Katsori, K. Dimas, D. J. Hadjipavlou-Litina, F. Pyleris, N. Sakellaridis and K. E. Litinas, Synthesis and biological evaluation of modified purine homo-*N*-nucleosides containing pyrazole or 2-pyrazoline moiety, *J. Enzyme Inhib. Med. Chem.*, 2014, **29**, 109–117.
56 G. L. Reddy, S. K. Guru, M. Srinivas, A. S. Pathania, P. Mahajan, A. Nargotra, S. Bhushan and R. A. Vishwakarma, Synthesis of 5-substituted-1*H*-pyrazolo[4,3-*d*]pyrimidin-7(6*H*)-one analogs and their biological evaluation as anticancer agents: mTOR inhibitors, *Eur. J. Med. Chem.*, 2014, **80**, 201–208.
57 A. M. A. Alnaja, T. A. Farghaly, H. S. A. El-zahabi and M. R. Shaaban, Cytotoxicity, docking study of new fluorinated fused pyrimidine scaffold: Thermal and microwave irradiation synthesis, *Med. Chem.*, 2021, **17**, 501–518.
58 E. V. Filho, J. W. S. Pina, M. K. Antoniazi, L. B. Loureiro, M. A. Ribeiro, C. B. Pinheiro, C. J. Guimaraes, F. C. E. de Oliveira, C. Pessoa, A. G. Taranto and S. J. Greco, Synthesis, docking, machine learning and antiproliferative activity of the 6-ferrocene/heterocycle-2-aminopyrimidine and 5-ferrocene-1*H*-pyrazole derivatives obtained by microwave-assisted Atwal reaction as potential anticancer agents, *Bioorg. Med. Chem. Lett.*, 2021, **48**, 128240.
59 P. H. Parikh, J. B. Timaniya, M. J. Patel and K. P. Patel, Microwave-assisted synthesis of pyrano[2,3-*c*]pyrazole derivatives and their anti-microbial, anti-malarial, anti-tubercular, and anti-cancer activities, *J. Mol. Struct.*, 2022, **1249**, 131605.
60 A. Dahal, M. Lo, S. Singh, H. Vo, D. ElHage, S. D. Jois and S. Murru, 1,3-Diarylpyrazolones as potential anticancer agents for non-small cell lung cancer: Synthesis and antiproliferative activity evaluation, *Chem. Biol. Drug Des.*, 2022, **99**, 620–633.
61 S. T. Boatenga, T. Roya, K. Torrey, U. Owunna, S. Banang-Mbeumi, D. Basnet, E. Niedda, A. D. Alexander, D. El Hage, S. Atchimnaidu, B. M. Nagalo, D. Aryal, A. Findley, N. P. Seeram, T. Efimova, M. Sechi, R. A. Hill, H. Ma, J. C. Chamcheu and S. Murru, Synthesis, *in silico* modelling, and *in vitro* biological evaluation of substituted pyrazole derivatives as potential anti-skin cancer, anti-

tyrosinase, and antioxidant agents, *J. Enzyme Inhib. Med. Chem.*, 2023, **38**, 2205042.

62 G. Mótyán, Á. Baji, M. A. Marc, M. K. Gopisetty, D. I. Adamecz, M. Kiricsi, É. A. Enyedy and É. Frank, Microwave-assisted synthesis, proton dissociation processes, and anticancer evaluation of novel D-ring-fused steroidal 5-amino-1-arylpyrazoles, *Appl. Sci.*, 2020, **10**, 229.

63 D. Ashok, M. R. Reddy, N. Nagaraju, R. Dharavath, K. Ramakrishna, S. Gundu, P. Shravani and M. Sarasija, Microwave-assisted synthesis and *in vitro* antiproliferative activity of some novel 1,2,3-triazole-based pyrazole aldehydes and their benzimidazole derivatives, *Med. Chem. Res.*, 2020, **29**, 699–706.

64 V. W. Y. Liao, A. Kumari, R. Narlawar, S. Vignarajan, D. E. Hibbs, D. Panda and P. W. Groundwater, Tubulin-binding 3,5-*bis*(styryl)pyrazoles as lead compounds for the treatment of castration-resistant prostate cancer, *Mol. Pharmacol.*, 2020, **97**, 409–422.

65 L. H. Al-Wahaibi, M. A. I. Elbastawesy, N. E. Abodya, B. G. M. Youssif, S. Bräse, S. N. Shabaan, G. H. Sayed and K. E. Answer, New pyrazole/pyrimidine-based scaffolds as inhibitors of heat shock protein 90 endowed with apoptotic anti-breast cancer activity, *Pharmaceuticals*, 2024, **17**, 1284.

66 S. M. H. Sanad and A. E. M. Mekky, New thieno[2,3-*b*] pyridine-fused pyrimidin-4(3*H*)-ones as potential thymidylate synthase inhibitors: Synthesis, SAR, *in vitro* and *in silico* study, *J. Mol. Struct.*, 2023, **1282**, 135236.

67 K. E. Anwer, S. S. A. El-Hddad, N. E. A. A. El-Sattar, A. El-morsy, F. Khedr, S. Mohamady, D. E. Keshek, S. A. Salama, K. El-Adl and N. S. Hanafy, Five and six membered heterocyclic rings endowed with azobenzene as dual EGFRT790M and VEGFR-2 inhibitors: Design, synthesis, *in silico* ADMET profile, molecular docking, dynamic simulation and anticancer evaluations, *RSC Adv.*, 2023, **13**, 35321–35338.

68 T. J. Mason, Ultrasound in synthetic organic chemistry, *Chem. Soc. Rev.*, 1997, **26**, 443–451.

69 G. Cravotto and P. Cintas, Power ultrasound in organic synthesis: Moving cavitational chemistry from academia to innovative and large-scale applications, *Chem. Soc. Rev.*, 2006, **35**, 180–196.

70 S. V. Sancheti and P. R. Gogate, A review of engineering aspects of intensification of chemical synthesis using ultrasound, *Ultrason. Sonochem.*, 2017, **36**, 527–543.

71 M. Draye, G. Chatel and R. Duwald, Ultrasound for drug synthesis: A green approach, *Pharmaceuticals*, 2020, **13**, 23.

72 N. S. Ahmed, K. O. AlFooty and S. S. Khalifah, Synthesis of 1,8-naphthyridine derivatives under ultrasound irradiation and cytotoxic activity against HepG2 cell lines, *J. Chem.*, 2014, **2014**, 1–8.

73 N. Suresh, B. V. Durgarao, A. Ratnakar, S. K. Kolli, M. A. Ashfaq, M. V. B. Rao and M. Pal, Ultrasound-Assisted 3-component reaction in acetic acid alone: Catalyst/promoter/ligand free synthesis of bioactive pyrazolo[1,5-*a*] pyrimidines, *Lett. Drug Des. Discovery*, 2017, **14**, 1176–1183.

74 T. D. Bhatt, D. G. Gojiya, P. L. Kalavadiya and H. S. Joshi, Rapid, greener and ultrasound irradiated one-pot synthesis of 4-(substituted-1*H*-pyrazol-4-yl)methylene)-3-isopropylisoxazol-5(4*H*)-ones and their *in vitro* anticancer activity, *ChemistrySelect*, 2019, **4**, 11125–11129.

75 G. M. Nitulescu, L. Matei, I. M. Aldea, C. Draghici, O. T. Olaru and C. Bleotu, Ultrasound-assisted synthesis and anticancer evaluation of new pyrazole derivatives as cell cycle inhibitors, *Arabian J. Chem.*, 2019, **12**, 816–824.

76 N. Nagasundaram, K. Padmasree, S. Santhosh, N. Vinoth, N. Sedhu and A. Lalitha, Ultrasound promoted synthesis of new azo fused dihydropyrano[2,3-*c*]pyrazole derivatives: *In vitro* antimicrobial, anticancer, DFT, *in silico* ADMET and molecular docking studies, *J. Mol. Struct.*, 2022, **1263**, 133091.

77 V. S. Dofe, A. P. Sarkate, S. V. Tiwari, D. K. Lokwani, K. S. Karnik, I. A. Kale, S. Dodamani, S. S. Jalalpure and P. V. L. S. Burra, Ultrasound assisted synthesis of tetrazole based pyrazolines and isoxazolines as potent anticancer agents via inhibition of tubulin polymerization, *Bioorg. Med. Chem. Lett.*, 2020, **30**, 127592.

78 N. M. Hassanin, T. E. Ali, M. A. Assiri and S. M. Abdel-Kariem, Novel carbazolyl–thiazolyl–chromone and carbazolyl–thiazolyl–pyrazole hybrids: Synthesis, cytotoxicity evaluation and molecular docking studies, *RSC Adv.*, 2024, **14**, 17245.

79 M. Leonardi, M. Villacampa and J. C. Menéndez, Multicomponent mechanochemical synthesis, *Chem. Sci.*, 2018, **9**, 2042–2064.

80 J.-L. Do and T. Friščić, Mechanochemistry: A force of synthesis, *ACS Cent. Sci.*, 2017, **3**, 13–19.

81 T. K. Achar, A. Bose and P. Mal, Mechanochemical synthesis of small organic molecules, *Beilstein J. Org. Chem.*, 2017, **13**, 1907–1931.

82 V. Martinez, T. Stolar, B. Karadeniz, I. Brekalo and K. Užarević, Advancing mechanochemical synthesis by combining milling with different energy sources, *Nat. Rev. Chem.*, 2023, **7**, 51–65.

83 H. R. M. Rashdan, S. M. Gomha, M. S. El-Gendey, M. A. El-Hashash and A. M. M. Soliman, Eco-friendly one-pot synthesis of some new pyrazolo[1,2-*b*]phthalazinediones with antiproliferative efficacy on human hepatic cancer cell lines, *Green Chem. Lett. Rev.*, 2018, **11**, 264–274.

84 M. M. Edrees, S. Abu-Melha, A. M. Saad, N. A. Kheder, S. M. Gomha and Z. A. Muhammad, Eco-Friendly synthesis, characterization and biological evaluation of some novel pyrazolines containing thiazole moiety as potential anticancer and antimicrobial agents, *Molecules*, 2018, **23**, 2970.